R. & M. No. 2710
(10,904)
A.R.C. Technical Report

MINISTRY OF SUPPLY

AERONAUTICAL RESEARCH COUNCIL
REPORTS AND MEMORANDA

Low-Speed Wind-Tunnel Tests on Two 45 deg Sweptback Wings of Aspect Ratios 4.5 and 3.0 (Models A and B)

By

J. TROUNCER, M.A.
and
G. F. MOSS, B.Sc.

LONDON: HER MAJESTY'S STATIONERY OFFICE
1953
PRICE 11s 6d NET

Low-Speed Wind-Tunnel Tests on Two 45 deg Sweptback Wings of Aspect Ratios 4.5 and 3.0 (Models A and B)

By

J. Trouncer, M.A.
and
G. F. Moss, B.Sc.

Communicated by the Principal Director of Scientific Research (Air),
Ministry of Supply

Reports and Memoranda No. 2710
June, 1947*

Summary.—Introduction.—A general programme of tests on sweptback wings is being made in the high and low-speed wind-tunnels of the Royal Aircraft Establishment to supplement existing data.

Range of Investigation.— Low-speed stability tests have been made on two wings of aspect ratio 4·5 and 3·0 (Models A and B). Both wings were of 45 deg sweepback, 4:1 taper ratio and 14 per cent thickness ratio.

The present report covers the tests made on these wings and is given in three parts :—

Part I Stability tests on the two wings without body or tail unit.

Part II ,, ,, ,, ,, ,, ,, with a body, fin and tailplane fitted (varying tail angle).

Part III Tests made with two types of nose flap on Model A (aspect ratio 4·5).

Results.—The results give the effect of aspect ratio on longitudinal, lateral and directional stability for a 'wing alone' and a wing, body and tail unit combination. They also give the value of the downwash at a constant distance behind the two wings.

The nose flaps tested on Model A did not prove effective as a means of improving the stability.

1. *Introduction.*—Before the advantages of sweepback at high Mach number were realised the only tests on sweptback wings were made on models of low-speed tailless aircraft where the sweepback did not normally exceed 40 deg and the aspect ratios were of the order of 6·0.

Since wings of larger sweepback and smaller aspect ratio are likely to be incorporated into many of the future aircraft designed to operate at high Mach number, a series of tests is being made in the high and low-speed wind-tunnels of the Royal Aircraft Establishment to supplement the existing data.

The low-speed tests are being made on four models :—

(1) Model A, sweepback 45 deg, aspect ratio 4·5.
(2) Model B, sweepback 45 deg, aspect ratio 3·0.
(3) Model C, sweepback 59 deg, aspect ratio 3·5.
(4) A half-wing model of Model A built for testing suction devices. The taper ratio of all these wings is 4:1 and the section is a 14 per cent thick symmetrical section.

The programme on Models A and B includes stability tests with and without a body and tail unit and some tests with nose flaps on Model A. The tests on Model C are mainly of pressure plotting to check the application of the linear perturbation theory. The half-wing model is being

* R.A.E. Report Aero 2210, received 8th October, 1947.

used to investigate the possibility of improving stability and maximum lift by applying suction in various ways.

2. *Range of Investigation.*—The present report gives the results of the tests made on Models A and B. These will be dealt with in three parts :—

(1) Tests on the wings without body or tail unit.

(2) Tests with body, fin and tailplane (varying tail angle).

(3) Tests with nose flaps on Model A.

All these tests were made in the No. 1, 11½-ft Wind Tunnel at a windspeed of 120 ft/sec. The corresponding Reynolds numbers (based on mean chord) are $1{\cdot}4 \times 10^6$ and $1{\cdot}7 \times 10^6$ for Models A and B respectively. A list of the symbols and definitions used in the report is attached.

Part I. Tests on Wings A and B without Body, Fin or Tailplane

3. *Details of Tests.*—Details of the two wings are given in Table 1 and the wing planforms are shown in Figs. 1a and 1b. Ordinates of the section used, a high-speed section designed by H. B. Squire, are given in Table 2. The original section was 10 per cent thick, but this was scaled up to 14 per cent to give a more reasonable value of the maximum lift coefficient at the Reynolds number of the tests.

Both wings were fitted with 20 per cent chord split flaps which covered 50 per cent of the span and were hinged in two alternative positions, at 60 per cent and 80 per cent of the chord. When open the angle along wind was 60 deg. Further details are given in Table 1.

The pitching moments for all tests on the wing alone are given about an axis through the mean quarter chord point of the wing.

4. *Range of Investigation.*—The tests included longitudinal stability measurements with flaps 0 deg and flaps 60 deg hinged in the two alternative positions and elevon angles of 0 deg and -10 deg. Lateral and directional stability measurements were also made over an incidence range with flaps 0 deg and flaps 60 deg hinged in the rear position.

5. *Results.*—The results of these tests provide a comparison between two wings of different aspect ratio, other factors being kept constant.

5.1. *Lift and Longitudinal Stability* (Tables 5 and 6, Figs. 4 to 12).—5.1.1. *Flaps 0 deg.*—The lift curves for the two wings are given in Figs. 4 and 5 and the basic curves with elevons 0 deg are shown compared in Fig. 10. The corresponding pitching-moment curves are given in Figs. 6, 8 and 11.

It will be seen that the reduction in aspect ratio from 4·5 to 3·0 causes a decrease in the lift slope at low angles of incidence from $dC_L/d\alpha = 0{\cdot}056$ per deg to $dC_L/d\alpha = 0{\cdot}052$ per deg. In both cases there is a change in slope of the lift curve at an incidence of about $\alpha = 18$ deg due to the development of a tip stall.

This tip stall is also evident from the pitching-moment curves particularly in the case of model A (aspect ratio 4·5) when the resulting instability is very pronounced above $C_L = 1{\cdot}0$. The wing of smaller aspect ratio (Model B) shows initial instability followed by increased stability just before the stall. No theoretical explanation has been advanced for this secondary stability, but it is consistent that it should occur on the wing of small aspect ratio if one considers the limiting case of a delta wing of the same taper ratio and approximately the same sweepback angle (46·5 deg) but with an aspect ratio of 1·33 (wing D.T. ¼ of Ref. 1). In this case the instability was eliminated altogether and there was an increase in stability at high lift coefficients (Fig. 6 of Ref. 1).

The changes in lift and pitching moment, flaps 0 deg, due to 10 deg of negative elevon angle are given below at two angles of incidence, showing the slight reduction in elevon effectiveness that occurs on both wings at high angles of incidence (Figs. 6 and 8).

TABLE A

ΔC_L and ΔC_M due to 10 deg of negative elevon angle

α deg	ΔC_L Model A	ΔC_L Model B	$\Delta C_{M0 \cdot 25\bar{c}}$ Model A	$\Delta C_{M0 \cdot 25\bar{c}}$ Model B
5	−0·09	−0·10	0·075	0·059
10	−0·07	−0·08	0·059	0·052

The neutral point at $C_L = 0$, flaps 0 deg, is given by $h_n = 0{\cdot}35$ for both wings, but at higher angles of incidence the neutral point on Model A is ahead of that on Model B. This result is surprising since, on a straight wing with no sweepback the neutral point tends to move back with increase of aspect ratio.

5.1.2. *Flaps 60 deg.*—The chief advantage obtained from opening the flaps is the reduction in the stalling angle from $\alpha = 27$ deg to $\alpha = 17$ deg or 18 deg. The actual gain in maximum lift is small or even negative (*see* Figs. 4 and 5), but the lift is obtained at a useable incidence.

Table B gives the lift increments and the values of maximum lift with flaps down for the two positions of the flap hinge line.

TABLE B

Lift increments and values of $C_{L\,\max}$ with flaps down (untrimmed values)

	Flaps hinged at 80 per cent chord		Flaps hinged at 60 per cent chord	
	C_L at $\alpha = 5$ deg	$C_{L\,\max}$	C_L at $\alpha = 5$ deg	$C_{L\,\max}$
Model A	0·48	1·32	0·36	1·15 approx.
Model B	0·44	1·31	0·31	1·17

Fig. 12, which is reproduced from Ref. 2, shows the order of decrease in maximum lift increment due to split flaps which may be expected with increasing angle of sweepback. The wings in this case had no taper and were of aspect ratio 4·8. It is clear from this that for wings of sweepback greater than 45 deg it is difficult to design a split flap that will give a positive increment in maximum lift.

The pitching-moment curves for the two flap positions are given in Figs. 7 and 9. From these and from Fig. 11 we can obtain the changes in trim due to the flaps at $\alpha = 5$ deg and the elevon angles required to trim out these changes assuming the elevon power to be linear up to $\eta_W = -20$ deg. These are given in Table C.

TABLE C

Changes in trim due to flaps and elevon angles required to retrim at $\alpha = 5$ deg

	Flaps hinged at 80 per cent chord		Flaps hinged at 60 per cent chord	
	$\Delta C_{M \cdot 25\bar{c}}$ due to flaps	$\Delta\eta_W$ deg to trim	$\Delta C_{M \cdot 25\bar{c}}$ due to flaps	$\Delta\eta_W$ deg to trim
Model A	−0·10	−12	−0·03	−4
Model B	−0·12	−21	−0·04	−7

The result of having to apply such large angles of elevon to trim out the negative pitching moment due to the flaps lessens the effective lift from the flaps considerably. The net increases in lift due to the flaps can be obtained from Tables A, B and C and are given below in Table D.*

TABLE D

Net increases in trimmed lift due to flaps at $\alpha = 5$ deg

	Flaps hinged at 80 per cent chord	Flaps hinged at 60 per cent chord
Model A	0·37	0·32
Model B	0·24	0·24

These figures show that on Model A the flaps at 80 per cent of the chord are more effective at a constant incidence while on Model B there is little to choose between the two positions. The same conclusion is reached if the values of maximum lift shown in Figs. 7 and 9 are considered.

The neutral point with flaps down is at about $0{\cdot}365\bar{c}$ in both cases at $\alpha = 0$ deg but, at higher incidences, as with the flaps up, the neutral point of Model A is ahead of that of Model B.

5.2. *Lateral and directional stability* (Tables 7 and 8, Figs. 13 to 19).—At low angles of incidence the yawing moments and rolling moments due to sideslip increased linearly. The values of n_v and l_v calculated between $\beta = \pm 5$ deg are plotted in Figs. 17 and 18. The sideforce measurements were small and tended to be scattered, but mean values of y_v have been plotted in Fig. 19 to give an indication of their order. The effect of aspect ratio was negligible except on n_v which, at angles of incidence above 9 deg showed higher values for the wing of smaller aspect ratio (Fig. 17).

At high angles of incidence, particularly on Model B the yawing moment and sideforce curves became very unsymmetrical and, at some angles of yaw unstable as shown by the curves of Figs. 13 and 14.

To investigate the cause of this a separate series of tests were made on Model B. The details of these tests have already been given in Ref. 3 and the results will only be summarized briefly here.

It was found that between $\alpha = 17$ deg and $\alpha = 19$ deg (the incidence at which the tip stall was evident from the change in slope of the lift curve) a secondary curve could be obtained of the type shown in Figs. 15 and 16. This effect was most evident on yawing moment, sideforce and drag and was caused by an early stall which occurred at the starboard tip if the model was disturbed. It was concluded from these tests that on any sweptback wing there is probably a critical incidence range of about 2 deg just below the tip-stalling incidence, over which range the lateral and directional curves will become unsymmetrical and unstable if disturbed. The result one would expect to obtain on a completely symmetrical wing in perfect flow would consist of a basic symmetrical curve and two alternative ' loops ' according as one or the other tip is caused to stall prematurely. On Model B one loop only could be obtained because of the tendency due to accumulative small errors, for the starboard wing tip to stall first even if undisturbed.

On Model A yawing moments were not measured beyond $C_L = 0{\cdot}88$ whereas the tip stall was not apparent from the lift curve until $C_L = 1{\cdot}0$. The only sign of asymmetry in this case was the increasingly large positive yaw at $\beta = 0$ deg (*see* Fig. 13).

Part II. Tests on Wings A and B with Body, Fin and Tailplane

6. *Details of Tests.*—The body used for these tests was circular in cross-section. The tailplane was 10 per cent thick, of aspect ratio 3·0 and with its quarter-chord line sweptback at 45 deg (*see* Table 1). The fin was equivalent to half the tailplane. Elevators were represented but no

* The values of ΔC_L due to elevon (flaps 0 deg) given in Table A can be assumed to apply for the flaps 60 deg case also.

rudders. A sketch of the body, fin and tailplane combination is shown in Fig. 2 and details of the body ordinates and of the tailplane section are given in Tables 2 and 3.

As the same body was used on both wings a greater portion of wing span was covered by the body in the case of Model B than Model A. The wing chord was set along the centre-line of the body and the position of the body relative to the wings was fixed by keeping the distance of the nose of the body ahead of the wing mean quarter-chord point the same in both cases.

The flaps used in these tests were the same as those used for the tests with wing alone, except that they were of reduced span to allow clearance for the body. The resulting flaps spans were 36 per cent and 32 per cent of the semi-span for Models A and B respectively. In each case only the rear position of flap was tested, *i.e.*, the hinge lines were at 80 per cent of the chord.

For the tests with body, all the pitching moments have been referred to $0{\cdot}45\bar{c}$ and, in cases where the curves for wing alone are needed for comparison, these have been transferred from $0{\cdot}25\bar{c}$ to the further aft c.g. This been done mainly to simplify the presentation of the results but also because the tunnel c.g. had to be moved to $0{\cdot}45\bar{c}$ for the tests with tailplane because of limitations on the balance.

The symbol η_E has been adopted throughout for elevator angles to avoid confusion with η_W which is the normal symbol for elevon angles on sweptback wings when these are defined along wind.

7. *Range of Investigation.*—Longitudinal measurements were made on the wings with body both with and without the fin and tailplane. The following tail settings relative to the body centre-line were used:—

Model A	Flaps 0 deg	$\eta_T = +\,1{\cdot}5$ deg, 0 deg and $-\,1{\cdot}4$ deg
	Flaps 60 deg	$\eta_T = +\,1{\cdot}5$ deg, 0 deg and $-\,1{\cdot}4$ deg
Model B	Flaps 0 deg	$\eta_T = 0$ deg, $-\,1{\cdot}4$ deg and $-\,2{\cdot}9$ deg
	Flaps 60 deg	$\eta_T = +\,1{\cdot}5$ deg, 0 deg, $-\,1{\cdot}4$ deg and $-\,2{\cdot}9$ deg

On Model A elevator angles of 0 deg, $-$ 5 deg, and $-$ 10 deg were tested at one tail setting ($\eta_T = 0$ deg).

Brief tests were also made to find the effect of the fin and tailplane on n_v, l_v and y_v at $C_L = 0$.

8. *Results.*—From these tests we can obtain the body effect and the mean downwash at a given distance behind the wing mean quarter-chord point for two wings of different aspect ratio.

8.1. *Lift and Longitudinal Stability* (Tables 9 and 10, Figs. 20 to 29).—8.1.1. *Effect of the body on stability.*—The body effect on lift is negligible for the wing of small aspect ratio, Model B (Fig. 21) but on Model A the body causes a slight increase in the value of $dC_L/d\alpha$ (Fig. 20).

The body effect on stability is also small in both cases. It causes a backward shift of the neutral point of $\Delta h_n = 0{\cdot}026$ in the case of Model A (Fig. 22) and of $\Delta h_n = 0{\cdot}010$ in the case of Model B (Fig. 23).

In a recent note[4] Professor Schlichting has given a simple theoretical method for calculating the neutral point shift due to a body on sweptforward and sweptback wings. In this he shows that the forward shift of about $\Delta h_n = 5$ per cent to 8 per cent of the mean chord that normally occurs with straight wing combinations is greatly increased when the wing is sweptforward and decreased when it is sweptback, becoming a backward shift if the angle of sweepback is great enough. The examples given in this note are based on two series of wings of aspect ratio 5 and taper ratios of 5:1 and 1:1 with the angle of sweepback varying from $-$ 30 deg to $+$ 45 deg. The results show that the small backward shift of the neutral point measured on Models A and B is consistent with theory and of the right order. It is clear from the tunnel results on the two wings that changes in aspect ratio give only relatively small changes in the movement of the neutral point due to the body.

8.1.2. *Effect of the tailplane on stability*.—The problem of longitudinal stability on a sweptback wing when this is part of a wing, body and tail unit combination is very different from the problems that arise when the wing is considered as an all-wing aircraft. For instance, the effect of a tip stall which is so serious on the longitudinal stability of the wing alone is overridden by the stable moment from the tailplane and is only evident by a slight decrease in the stability at some incidences.

This does not mean that such a tip stall can be tolerated on a wing, body and tail unit combination since it will still seriously affect both the aileron power and the lateral stability of the aircraft. The pitching-moment curves for Models A and B with body and tailplane are plotted in Figs. 22 and 23 (flaps 0 deg) and in Figs. 24 and 25 (flaps 60 deg) for various tail settings. The neutral point positions obtained from these curves are $h_n = 0{\cdot}55$ and $h_n = 0{\cdot}45$ for Models A and B respectively with an increasing backward shift, particularly on Model B as the lift coefficient increases up to the tip stalling incidence. Comparison of Figs. 11 and 26 shows that, the backward shift of the neutral point due to the tailplane is considerably more for Model A than for Model B, this being due to the larger downwash that occurs at the tailplane behind Model B (*see* section 8·13).

The effect of elevator movements of 5 deg and 10 deg on the pitching moment curves for Model A are given in Fig. 22. Over the range $\alpha = 0$ deg to $\alpha = 15$ deg the mean increments in lift and pitching moment due to 10 deg of negative elevator are $\Delta C_L = -0{\cdot}064$ and $\Delta C_M = 0{\cdot}165$.

8.1.3. *Downwash*.—The mean downwash behind the two wings at the tailplane position has been calculated over the incidence ranges $\alpha = 0$ deg to $\alpha = 16$ deg (flaps 0 deg) and $\alpha = 0$ deg to $\alpha = 17{\cdot}5$ deg (flaps 60 deg). The results for the two cases are shown plotted in Figs. 27 and 28 and the values of $d\varepsilon/d\alpha$ at low incidences are given below in Table E.

TABLE E

Downwash at the tailplane position

	$d\varepsilon/d\alpha$	
	Flaps 0 deg	Flaps 60 deg (hinged at 80 per cent chord)
Model A	0·55	0·55
Model B	0·59	0·63

These values of $d\varepsilon/d\alpha$ are rather surprisingly large in view of the only German data available on the downwash behind sweptback wings. In a series of tests on wings of aspect ratio 5·0 H. Trienes[5] obtained the variation of $d\varepsilon/d\alpha$ with angle of sweepback shown in Fig. 29. It will be seen that from these curves the downwash one would expect to obtain behind Model A would be of the order of $d\varepsilon/d\alpha = 0{\cdot}43$. The higher value actually obtained is probably due to the effect of the body on Model A there being no body present in the German tests.

The reduction in $d\varepsilon/d\alpha$ with angle of sweepback shown in Fig. 29 is due to the fact that sweepback causes a reduction in the lift loading at the centre of the wing and an increase at the tips. The higher value of $d\varepsilon/d\alpha$ obtained on Model B compared with Model A is due to the normal effect of a decrease of aspect ratio on downwash.

8.2. *Lateral and Directional Stability* (Tables 11 and 12).—The values of n_v, l_v and y_v at $C_L = 0$ were measured on the two wings with body both with and without the tail unit. Comparison with the results for wing alone (allowing for the change of c.g. position) gives the following table of increments.

TABLE F

Effect of body and tail unit on n_v, l_v and y_v (c.g. at $0{\cdot}45\bar{c}$)

		Δn_v	Δl_v	Δy_v
Body	Model A	—0·066		—0·029
	Model B	—0·076	—0·005	—0·019
Fin and tailplane	Model A	0·159		—0·141
	Model B	0·187	—0·014	—0·127

It can be assumed that these increments will be roughly constant over the incidence range at least up to the tip stall and the curves of n_v, l_v and y_v with body and tail unit can be obtained from the curves for wing alone of Figs. 17, 18 and 19 if correction is made to the yawing and rolling moments for the change in c.g. position.*

Part III. Tests with Nose Flaps on Model A

9. *Introduction.*—On the tailless aircraft of Ref. 6, which had a 10 per cent thick wing swept-back at 40 deg, tests showed that nose flaps were an effective means of ensuring stability over the whole incidence range. It was decided, therefore, to try the effect of similar nose flaps on Model A.

10. *Details of Tests.*—Two types of nose flap were tested :—

(a) Flat plate nose flaps of constant chord (1·81 in.) set at an angle of 135 deg to the wing chord (*see* Fig. 3a).

(b) Nose flaps of similar chord but curved to fair into the wing surface and set at an angle to the wing chord which varied along the span, ranging from 140 deg at the tip to 125 deg at 50 per cent of the span (*see* Fig. 3b).

These angles were chosen by the aid of the German results on nose flaps given in Ref. 7.

Both types of nose flap were designed to extend inboard from the tip to cover 40 per cent or 50 per cent of the span.

The pitching moments for these tests are all given relative to the mean quarter-chord point of the wing to provide direct comparison with the ' wing alone ' results without nose flaps.

11. *Range of Investigation.*—Longitudinal measurements with nose flaps fitted were made on the wing alone and on the wing and body both with flaps 0 deg and with flaps 60 deg hinged at 80 per cent of the chord.

12. *Results* (Table 13, Figs. 30, 31).—The initial tests were made with the flat plate type of nose flap, similar to the type described in Ref. 6. It was found, however, that on Model A these gave no improvement to the stalling characteristics as can be seen from the curves of Fig. 31. It seemed probable that this might be due to the thicker section of Model A (14 per cent as compared with 10 per cent) causing too sudden a change of curvature at the junction of the wing and nose flap. It was also thought that the use of a constant angle combined with a constant chord nose flap might be proving too great a simplification since it was known from German tests that the optimum setting varies with the chord length and, in the case of Model A the nose flap-chord/local-chord ratio varied from 20 per cent at the tip to 8 per cent at 50 per cent of the span.

---

* The values of n_v and l_v about $0{\cdot}45\bar{c}$ for the ' wing alone ' cases are given by the equations

Model A $\quad (n_v)_{0\cdot45\bar{c}} = (n_v)_{0\cdot25\bar{c}} + 0{\cdot}090 \cos\alpha \times y_v$

$\quad (l_v)_{0\cdot45\bar{c}} = (l_v)_{0\cdot25\bar{c}} + 0{\cdot}090 \sin\alpha \times y_v$

Model B $\quad (n_v)_{0\cdot45\bar{c}} = (n_v)_{0\cdot25\bar{c}} + 0{\cdot}134 \cos\alpha \times y_v$

$\quad (l_v)_{0\cdot45\bar{c}} = (l_v)_{0\cdot25\bar{c}} + 0{\cdot}134 \sin\alpha \times y_v$

For these reasons the second type of nose flap was developed, with a curved surface faired into the wing and an angle to the wing chord which varied along the span and was designed to give the optimum setting at each point, based on the ratio of nose flap chord/local chord.

Tests made with this second type of nose flap showed that, although they increased the maximum lift obtainable with positive stability by $\Delta C_L \simeq 0 \cdot 12$, the wing still became unstable at the final stall. Observation of the flow with tufts showed that, even with the nose flaps fitted, there was still considerable outflow near the trailing edge at the tip and there was also a breakaway which tended to form off the inboard end of the nose flap.

An upper surface fin of the type shown in Fig. 1a was fitted along the chord at 50 per cent of the span to check the outflow and the inboard end of the nose flap was faired into the wing. Although the fin changed the form of the pitching-moment curve it gave no improvement in the stalling characteristics of the wing (Fig. 31).

The body effect with nose flaps was again very small.

In view of these results one can only conclude that there is a limit to the type of sweptback wings for which effective nose flaps can be designed. Although they proved successful on the aircraft of Ref. 6 there are differences between that model and Model A, *i.e.*, increased wing thickness, higher taper and greater sweepback, all of which tend to make the tip stall more severe and so increase the difficulty of finding any effective means of delaying it.

A further difference between the two models is the design of the wing body junction. On the aircraft of Ref. 6 the wing near the body was thickened up to include entries and, as a result, the root stalled at about $\alpha = 18$ deg, whereas, on Model A the root is still unstalled by $\alpha = 26$ deg. This means that, if a stable stall is to be achieved on Model A then the tip stall must be delayed to a considerably higher angle of incidence than was necessary on the other model.

There is no evidence from German tests to suggest that the results obtained on Model A are pessimistic or that the Germans themselves have designed an efficient nose flap on a comparable wing. The systematic German tests on nose flaps were mostly made on straight wings, apart from the tests reported in Ref. 7 which were made on a 10 per cent to 12 per cent thick wing of only 35 deg sweepback, and which are, therefore, hardly comparable. Some tests with nose flaps were made on a highly tapered thick wing of 45 deg sweepback[8], but for these tests the nose flaps covered the whole span and were considered as a means of increasing the maximum lift rather than as a means of improving the stability and no pitching-moment curves are included in the report.

It seems probable, therefore, that on highly tapered wings of large sweepback such as Models A and B some new means of curing the tip stall will have to be employed if these wings are to be a practical proposition at low speeds.

List of Symbols and Definitions

S	Wing area $= \frac{1}{2} \times b(c_r + c_t)$
b	Wing span (tip chord to tip chord)
$\bar{c}$	Mean chord $= S/b$
A	Aspect ratio $= b/\bar{c}$
c_r	Root chord, *i.e.*, chord on centre-line
c_t	Tip chord
S'	Tailplane area $= \frac{1}{2} \times b'(c_r' + c_t')$ *N.B.* This is not the standard definition
b'	Tailplane span (tip chord to tip chord)
c_r'	Tailplane chord on centre-line
c_t'	Tailplane tip chord
V	Tunnel speed
ρ	Air density
α deg	Incidence of wing chord line and body centre-line
β deg	Angle of sideslip
C_L	Lift$/\frac{1}{2}\rho V^2 S$
C_D	Drag$/\frac{1}{2}\rho V^2 S$
C_M	Pitching moment$/\frac{1}{2}\rho V^2 S \bar{c}$
C_n	Yawing moment$/\frac{1}{2}\rho V^2 Sb$
C_l	Rolling moment$/\frac{1}{2}\rho V^2 Sb$
C_Y	Side force$/\frac{1}{2}\rho V^2 S$
n_v	$dC_n/d\beta$ (β in radians)
l	$dC_l/d\beta$,,
y_v	$\frac{1}{2} \times dC_Y/d\beta$,,
η_W deg	Elevon angle (defined in a chordwise direction)
η_E deg	Elevator angle (defined in a chordwise direction)
η_T deg	Angle of tailplane relative to wing chord and body centre-line
ε deg	Mean downwash at mean quarter-chord of tailplane
h_n	Neutral point position as percentage of mean chord

N.B. The same wing area has been used for the tests with and without body (applies to C_L, C_D, C_M, C_n, C_l, C_Y)

REFERENCES

No.	*Author*	*Title, etc.*
1	M. Gdaliahu	A Summary of the Results of some German Model Tests on Wings of Small Aspect Ratio. A.R.C. Report 9638. (Unpublished.)
2	M. Hansen	Dreikomponentenmessungen an Pfeilflügeln mit Spreizklappe. F.B. 1626.
3	J. Trouncer	Wind Tunnel Tests to Investigate Directional Asymmetry and Instability on a Sweptback Wing (Model B 45 deg Sweepback Aspect Ratio 3). A.R.C. 10,489. (Unpublished.)
4	H. Schlichting	Calculation of the Influence of a Body on the Position of the Aerodynamic Centre of Aircraft with Sweptback Wings. R. & M. 2852. March, 1947.
5	H. M. Lyon	Abstract from 'Systematic Measurements of Downwash Behind Sweptback Wings' by Hans Trienes. A.I.T.H.B. Report 45/8. A.R.C. Report 9959.
6	J. Trouncer	A Comparison of the Effects of Slats, Nose Flaps and Double Split Flaps on a Model of a 40 deg Sweptback Tailless Aircraft. A.R.C. Report 9980. (Unpublished.)
7	W. Krüger	Windkanaluntersuchungen an einem 35 deg Pfeilflügel mit verscheidenen Landehilfen.
8	W. Krüger	Windkanalmessungen an einem 45 deg Pfeil-Trapezflügel mit Nasenklappe. U. & M. 3155.

TABLE 1

Model Data

	Model A	Model B
Wing		
area S	16·07 sq ft	
span b	8·5 ft	6·94 ft
mean chord $\bar{c}$	1·891 ft	2·313 ft
aspect ratio A	4·5	3·0
sweepback (quarter-chord line)	45 deg	
taper c_r/c_t	4:1	
*thickness/chord ratio	14 per cent	
root chord c_r	3·024 ft	3·700 ft
tip chord c_t	0·756 ft	0·925 ft
Position of mean quarter-chord point distance back from L.E.R.C.	2·456 ft	2·313 ft
Elevons span(each) 50 per cent of semi-span, *i.e.*,	2·13 ft	1·74 ft
area aft of hinge (each)	0·710 sq ft	0·705 sq ft
chord aft of hinge (constant)	0·332 ft	0·406 ft
Split flaps (a) For wing alone tests		
angle (chordwise)	60 deg	
hinge line (forward position)	60 per cent local chord	
(rear position)	80 per cent local chord	
span (each) 50 per cent semi-span, *i.e.*	2·13 ft	1·74 ft
chord	20 per cent local chord	
area (each)	1·045 sq ft	1·043 sq ft
(b) For tests with body angle, chord and hinge line position as above		
span (each)	1·52 ft	1·12 ft
area (each)	0·697 sq ft	0·619 sq ft
***Body*†**		
length	9·96 ft	
maximum diameter	1·25 ft	
Tailplane		
area S' defined as $b'/2\ (c_r' + c_t')$	3·57 sq ft	
span b'	3·30 ft	
aspect ratio	3·05	
sweepback (quarter-chord line)	45 deg	
taper c_r'/c_t'	1·84:1	
‡thickness ratio	10 per cent	
chord on centre-line c_r'	1·40 ft	
tip chord c_t'	0·76 ft	
position of mean quarter-chord point, distance back from L.E. of centre-line chord	1·09 ft	
tail arm l (mean quarter-chord wing to mean quarter-chord tail)	5·35 ft	
Elevators span (each)	1·31 ft	
area aft of hinge (each)	0·664 sq ft	
chord aft of hinge	50 per cent local chord	

* Ordinates of the wing section are given in Table 2.
† Ordinates of the body are given in detail in Table 3.
‡ Ordinates of the tailplane section are given in Table 4.

Fin *Model A* *Model B*

This is equivalent to half the tailplane set in a vertical plane with its centre-line chord coinciding with the centre-line chord of the tailplane.

net area (*i.e.*, area outside the body) .. .. 1·247 sq ft

Nose Flaps (for Model A only)—details given in Figs. 3a and 3b

Upper Surface Fin (for Model A only)
position—along rearmost 67 per cent of chord at 50 per cent span
area (each) .. .. 0·32 sq ft

N.B. The areas of the wings and tailplane are the areas between the two tip chords, *i.e.*, ignoring the radiused tip. The mean chords and spans, etc., are given with the same convention.

TABLE 2

Ordinates of Wing Section for Models A and B

14 *per cent Thick Symmetrical Section* (*Section B of Aero Memorandum* 27)

Distance from L.E. (per cent chord)	Half ordinate (per cent chord)
0	0
0·5	1·219
0·75	1·490
1·25	1·916
2·5	2·684
5·0	3·723
7·5	4·468
10	5·050
15	5·908
20	6·483
25	6·839
30	6·996
35	6·935
40	6·721
45	6·392
50	5·974
55	5·486
60	4·943
65	4·362
70	3·753
75	3·130
80	2·504
85	1·878
90	1·252
95	0·626
100	0

Nose radius = 1·5 per cent chord.

TABLE 3

Ordinates of Body for Models A and B

Distance from nose (in.)	Body radius (in.)
0	0
0·573	1·040
1·720	1·800
2·868	2·323
5·735	3·268
11·470	4·545
17·205	5·423
22·940	6·065
28·675	6·535
34·413	6·905
40·148	7·168
45·883	7·350
51·618	7·463
57·353	7·500
63·088	7·463
68·823	7·345
74·558	7·138
80·293	6·833
86·028	6·423
91·763	5·900
97·500	5·245
103·233	4·400
108·970	3·063
119·480	0

TABLE 4

Ordinates of Tailplane Section for Models A and *B*

10 *per cent Thick Symmetrical Section*

Distance from L.E. (per cent chord)	Half ordinate (per cent chord)
0	0
0·5	0·863
0·75	1·059
1·25	1·357
2·5	1·911
5·0	2·655
7·5	3·190
10	3·601
15	4·214
20	4·625
25	4·881
30	5·000
35	4·964
40	4·803
45	4·565
50	4·274
55	3·916
60	3·524
65	3·107
70	2·774
75	2·244
80	1·792
85	1·339
90	0·887
95	0·452
100	0

TABLE 5

Lift, Drag and Pitching-Moment Coefficients on Model A

Wing alone, *i.e.*, no body or tail unit

$\eta_W = 0$ deg				$\eta_W = -10$ deg			
α deg	C_L	C_D	$C_{M\,0\cdot25\bar{c}}$	α deg	C_L	C_D	$C_{M\,0\cdot25\bar{c}}$
Flaps 0 *deg*							
0·3	0·11	0·0072	+0·0015	4·5	0·183	0·0119	+0·0520
4·6	0·283	0·0137	−0·0261	8·8	0·439	0·0255	+0·0218
8·9	0·523	0·0312	−0·0426	13·1	0·694	0·0545	−0·0040
11·0	0·630	0·0430	−0·0465	15·25	0·824	0·0842	−0·0245
13·15	0·747	0·0623	−0·0540	17·35	0·933	0·1297	−0·0242
15·3	0·885	0·0979	−0·0703	19·45	1·014	0·1768	−0·0069
17·45	1·000	0·1439	−0·0732	21·5	1·086	0·2474	+0·0091
19·5	1·083	0·1990	−0·0577	23·6	1·142	0·3080	+0·0177
21·6	1·155	0·2533	−0·0440	25·65	1·190	0·3691	+0·0234
23·7	1·222	0·3224	−0·0356	26·65	1·199	0·4025	+0·0295
25·3	1·253	0·3823	−0·0348				
26·25	1·280	0·4242	−0·0302				
26·75	1·280	0·4485	−0·0207				
Flaps 60 *deg* (*hinged at* 80 *per cent chord*)							
0·95	0·557	0·0952	−0·1012	0·8	0·450	0·1020	−0·0122
5·2	0·802	0·1185	−0·1292	5·1	0·696	0·1192	−0·0443
9·45	1·032	0·1504	−0·1473	9·35	0·948	0·1467	−0·0766
13·7	1·246	0·2241	−0·1575	13·65	1·178	0·2080	−0·1077
15·75	1·304	0·2821	−0·1392	17·7	1·246	0·3338	−0·0528
17·8	1·318	0·3628	−0·0918				
19·75	1·300	0·4218	−0·0739				
Flaps 60 *deg* (*hinged at* 60 *per cent chord*)							
0·8	0·438	0·0953	−0·0283	0·7	0·342	0·1023	0·0528
5·05	0·669	0·1085	−0·0568	4·95	0·567	0·1098	0·0215
9·3	0·873	0·1295	−0·0748	9·2	0·788	0·1262	−0·0093
13·5	1·071	0·1751	−0·0923	13·45	1·020	0·1652	−0·0459
15·55	1·130	0·2168	−0·0786	17·55	1·105	0·2569	−0·0089
17·6	1·157	0·2695	−0·0448				

TABLE 6

Lift, Drag and Pitching-Moment Coefficients on Model B

Wing alone, *i.e.*, no body or tail unit

$\eta_W = 0$ deg				$\eta_W = -10$ deg			
α deg	C_L	C_D	$C_{M\,0\cdot25\bar{c}}$	α deg	C_L	C_D	$C_{M\,0\cdot25\bar{c}}$
0·35	0·026	0·0067	−0·0041	0·2	−0·076	0·0101	0·0565
*2·45	0·150	0·0093	−0·0165	4·45	0·155	0·0115	0·0359
4·6	0·257	0·0143	−0·0255	8·7	0·382	0·0259	0·0117
8·8	0·483	0·0345	−0·0459	12·95	0·616	0·0537	−0·0150
13·05	0·695	0·0657	−0·0644	15·1	0·738	0·0747	−0·0371
15·2	0·811	0·0891	−0·0825	17·25	0·858	0·102	−0·0573
17·3	0·939	0·121	−0·1098	19·35	0·947	0·158	−0·0662
19·4	1·021	0·181	−0·1120	21·4	1·000	0·219	−0·0646
21·45	1·060	0·244	−0·1028	23·45	1·048	0·280	−0·0707
23·5	1·104	0·303	−0·1074	25·5	1·082	0·342	−0·0785
25·55	1·129	0·367	−0·1130	27·5	1·098	0·431	−0·0799
27·55	1·155	0·467	−0·1178				
28·55	1·144	0·489	−0·1219				
Flaps 60 *deg* (*hinged at* 80 *per cent chord*)							
0·85	0·512	0·106	−0·1269	0·75	0·420	0·123	−0·0695
5·1	0·731	0·134	−0·1521	5·0	0·633	0·135	−0·0916
9·35	0·946	0·172	−0·1776	9·2	0·850	0·167	−0·1181
13·55	1·162	0·221	−0·2054	13·45	1·074	0·210	−0·1518
15·65	1·264	0·248	−0·2234	15·6	1·181	0·237	−0·1730
16·75	1·312	0·265	−0·2268	17·6	1·204	0·309	−0·1665
17·6	1·211	0·369	−0·1768	19·55	1·171	0·378	−0·1433
Flaps 60 *deg* (*hinged at* 60 *per cent chord*)							
0·75	0·393	0·106	−0·0449				
4·95	0·597	0·123	−0·0683				
9·15	0·785	0·147	−0·0899				
13·35	0·978	0·178	−0·1123				
15·45	1·065	0·200	−0·1293				
16·5	1·123	0·213	−0·1387				
17·05	1·141	0·219	−0·1431				
17·6	1·174	0·234	−0·1140				
18·5	1·103	0·279	−0·1117				

* The measurements at this incidence were taken at a later date

TABLE 7

Lateral and Directional Coefficients and Derivatives on Model A

Wing alone, *i.e.*, no body or tail unit

(c.g. at $0{\cdot}25\bar{c}$)

α deg	C_L ($\beta = 0$ deg)	β deg	$10^3 C_n$	$10^3 C_Y$	$10^3 C_l$	n_v	y_v	l_v
Flaps 0 deg								
		10	0·10	−1·0	−3·70			
		5	0·08	−0·4	−3·58			
0·3	0·007	0	0·02	0	−2·89	0·001	−0·003	−0·008
		−5	−0·05	0·6	−2·20			
		−10	−0·12	1·2	−1·84			
		15	1·24	−1·4	−20·16			
		10	0·83	0	−14·95			
		5	0·28	0·5	−9·12			
4·6	0·287	0	−0·37	1·0	−3·32	0·006	−0·004	−0·067
		−5	−0·81	1·7	2·61			
		−10	−1·35	2·2	8·84			
		−15	−1·84	3·1	14·96			
		10	3·33	−1·4	−22·93			
		5	1·57	−0·4	−12·62			
8·9	0·523	0	−0·30	0·6	−0·99	0·021	−0·004	−0·132
		−5	−2·05	1·1	10·36			
		−10	−3·67	1·8	20·72			
		10	4·52	−2·5	−24·01			
		5	2·27	−2·5	−11·90			
11·0	0·635	0	0·54	−1·7	0·89	0·023	−0·003	−0·141
		−5	−1·66	−1·5	12·67			
		−10	−3·44	−0·7	22·78			
		10	5·25	−3·9	−20·80			
		5	3·17	−4·6	−9·72			
13·15	0·750	0	1·68	−5·7	1·22	0·016		−0·126
		−5	0·35	−5·8	12·33			
		−10	−1·64	−4·9	21·66			
		15	6·76	−7·5	−24·60			
		10	5·70	−8·9	−12·31			
		5	4·80	−10·2	−4·97			
15·3	0·872	0	3·48	−8·2	2·41	0·014		−0·080
		−5	2·30	−6·7	9·05			
		−10	0·93	−5·8	14·98			
		−15	−4·07	−2·3	29·79			

TABLE 7—*continued*

α deg	C_L (β = 0 deg)	β deg	$10^3 C_n$	$10^3 C_Y$	$10^3 C_l$	n_v	y_v	l_v
Flaps 60 deg (hinged at 80 per cent chord)								
		10	2·86	−7·2	−21·23			
		5	0·85	−3·1	−11·37			
2·0	0·620	0	−0·59	−0·4	−1·25	0·018	−0·016	−0·116
		−5	−2·24	2·4	8·95			
		−10	−4·31	6·4	19·59			
		15	7·92	−14·1	−41·11			
		10	5·22	−9·3	−27·71			
		5	2·15	−4·5	−14·35			
5·2	0·805	0	−0·54	−2·0	−0·62	0·032	−0·020	−0·162
		−5	−3·43	2·4	13·94			
		−10	−6·87	7·2	28·29			
		−15	−9·69	12·6	41·79			
		10	8·63	−11·2	−33·46			
		5	3·93	−7·4	−16·90			
9·45	1·070	0	−0·06	−3·6	0·69	0·048	−0·024	−0·201
		−5	−4·54	1·1	18·18			
		−10	−8·75	5·4	34·88			
		15	14·64	−16·4				
		10	9·53	−9·7	−33·06			
		5	5·12	−6·9	−15·86			
		2·5	4·34	−6·5				
11·5	1·146	0	3·75	−8·9	0·74			
		−5	−1·12	−4·5	18·63			
		−10	−6·92	2·0	34·34			

TABLE 8

Lateral and Directional Coefficients and Derivatives on Model B

Wing alone, *i.e.*, no body or tail unit

(c.g. at $0 \cdot 25\bar{c}$)

α deg	C_L ($\beta = 0$ deg)	β deg	$10^3 C_n$	$10^3 C_Y$	$10^3 C_l$	n_v	y_v	l_v
Flaps 0 deg								
		15	−0·29	−1·7	−4·4			
		10	−0·20	−1·1	−4·0			
		5	−0·13	−0·4	−3·4			
0·35	0·025	0	0·01	0·2	−2·7	−0·001	−0·002	−0·006
		−5	−0·02	0·4	−2·4			
		−10	0·06	0·8	−1·6			
		−15	0·06	1·8	−0·6			
		10	1·27	0·6	−16·0			
		5	0·68	1·3	−9·2			
5·65	0·314	0	−0·05	2·2	−1·8	0·009	−0·006	−0·083
		−5	−0·88	3·3	5·4			
		−10	−1·42	3·7	12·8			
		10	4·83	1·1	−26·3			
		5	2·47	2·0	−14·3			
10·95	0·598	0	−0·07	3·9	−0·8	0·031	−0·007	−0·156
		−5	−2·88	4·4	12·8			
		−10	−5·28	5·6	25·4			
		10	7·06	−0·6	−26·1			
		5	3·47	2·0	−13·3			
14·15	0·763	0	0·36	2·6	−0·6	0·037	−0·009	−0·146
		−5	−3·06	5·0	12·1			
		−10	−7·00	7·3	25·8			
		10	8·16	−2·9	−25·3			
		5	4·11	−1·1	−10·0			
16·25	0·880	0	0·27	3·4	−1·4	0·047	−0·024	−0·113
		−5	−4·04	7·4	9·7			
		−10	−7·00	6·0	25·0			
		15	11·14	−0·9	−39·4			
		10	7·91	−1·7	−24·8			
		5	5·06	−3·2	−10·3			
17·05	0·939	0	−0·49	4·2	−0·6	—	—	—
		−2·5	−2·16	6·4				
		−5	−1·40	1·6	11·8			
		−10	−6·03	4·7	25·1			
		−15	−10·01	3·7	42·1			

TABLE 8—*continued*

α deg	C_L ($\beta = 0$ deg)	β deg	10^3C_n	10^3C_Y	10^3C_l	n_v	y_v	l_v
Flaps 0 deg—continued		15	11·88	−2·2	−39·2			
		12·5	11·55	—	—			
		10	11·47	−9·4	−19·8			
		7·5	14·46	−23·5	−4·1			
		5	13·59	−29·6	5·6			
19·4	1·028	0	12·06	−30·3	16·9			
		−5	4·68	−16·2	21·5			
		−10	−2·09	−4·8	29·7			
		−15	−10·55	4·7	41·7			
Flaps 60 deg (hinged at 80 per cent chord)								
		15	2·79	−5·5	−26·3			
		10	1·85	−1·6	−17·2			
		5	0·97	−0·4	−10·1			
0·85	0·510	0	0·31	1·1	−2·6	0·008	−0·008	−0·090
		−5	−0·35	2·4	5·7			
		−10	−1·23	5·2	13·5			
		−15	−2·58	8·5	22·3			
		10	5·02	−3·3	−29·5			
		5	2·63	0·4	−15·3			
6·15	0·787	0	−0·42	4·2	−1·3	0·032	−0·018	−0·158
		−5	2·91	6·9	12·1			
		−10	5·80	10·1	26·3			
		10	11·34	−6·0	−38·2			
		5	5·67	−0·5	−20·6			
11·45	1·06	0	0·66	2·6	−0·3	0·065	−0·031	−0·226
		−5	−5·75	10·3	18·8			
		−10	−11·17	14·8	38·7			
		10	14·41	−6·2	−39·1			
		5	7·73	−1·2	−20·5			
14·6	1·206	0	0·90	4·9	−0·7	0·084	−0·034	−0·230
		−5	−6·87	10·7	19·8			
		−10	−13·48	13·4	40·7			

TABLE 9a

Lift, Drag and Pitching-Moment Coefficients on Model A with Body and Fin

No tailplane

α deg	C_L	C_D	$C_{M\,0\cdot45\bar{c}}$
Flaps 0 deg			
0·35	0·027	0·0131	0·0025
3·55	0·216	0·0167	0·0209
6·75	0·417	0·0284	0·0406
10·0	0·607	0·0461	0·0641
13·2	0·784	0·0743	0·0840
16·4	0·982	0·134	0·1038
19·6	1·136	0·213	0·1520
21·65	1·210	0·257	0·1836
23·7	1·248	0·334	0·2130
25·7	1·256	0·409	0·2335
26·75	1·267		
27·75	1·267	0·489	0·2423
Flaps 60 deg (hinged at 80 per cent chord)			
0·75	0·408	0·0769	−0·0192
2·9	0·541	0·0832	−0·0185
5·05	0·669	0·0943	−0·0072
9·35	0·912	0·123	0·0186
13·6	1·158	0·180	0·0425
15·7	1·233	0·228	0·0763
17·75	1·290	0·276	0·1100
19·75	1·295	0·337	0·1586
21·7	1·223	0·401	0·1872

TABLE 9b

Lift, Drag and Pitching-Moment Coefficients on Model A with Body and Fin

With tailplane

η_T deg	η_E deg (Elevators)	α deg	C_L	C_D	$C_{M\,0\cdot45\bar{c}}$
Flaps 0 deg					
0	0	0·35	0·010	0·0144	0·0047
		3·55	0·240	0·0188	−0·0173
		6·75	0·463	0·0321	−0·0398
		10·0	0·654	0·0519	−0·0593
		13·2	0·874	0·0867	−0·0903
		16·4	1·098	0·155	−0·1328
		19·6	1·280	0·241	−0·162
		21·65	1·375	0·307	−0·209
		23·7	1·418	0·397	−0·262
		25·7	1·450	0·486	−0·296
		27·75	1·480	0·587	−0·344
0	−5	3·55	0·210	0·0187	0·0664
		6·75	0·422	0·0303	0·0444
		10·0	0·621	0·0484	0·0282
		13·2	0·830	0·0805	0·0012
		16·4	1·062	0·146	−0·0392
		19·6	1·228	0·230	−0·0606
		22·65	1·363	0·332	−0·1384
		25·7	1·419	0·472	−0·226
		28·75	1·460	0·604	
0	−10	3·55	0·179	0·0198	0·1497
		10·0	0·591	0·0467	0·1048
		13·2	0·807	0·0785	0·0748
		16·4	1·030	0·144	0·0422
		19·6	1·196	0·222	0·0254
		22·65	1·330	0·323	−0·044
		25·7	1·393	0·463	−0·152
−1·4	0	0·35	0·016	0·0145	0·0340
		3·55	0·234	0·0186	0·0153
		6·75	0·434	0·0303	−0·0018
		10·0	0·635	0·0502	−0·0191
		13·2	0·854	0·0843	−0·0507
		16·4	1·080	0·152	−0·0877
		19·6	1·247	0·233	−0·1028
		22·65	1·371	0·340	−0·1845
		25·7	1·445	0·484	

Table 9b—*continued*

η_T deg	η_E deg (Elevators)	α deg	C_L	C_D	$C_{M\,0\cdot45\bar{c}}$
Flaps 0 *deg—continued*					
1·5	0	0·35	0·037	0·0145	—0·0399
		3·55	0·255	0·0195	—0·0625
		6·75	0·475	0·0338	—0·0857
		10·0	0·679	0·0549	—0·1072
		13·2	0·894	0·0919	—0·1494
		16·4	1·138	0·167	—0·196
		19·6	1·295	0·254	—0·227
		22·65	1·423	0·365	—0·286
Flaps 60 *deg* (*hinged at* 80 *per cent chord*)					
0	0	0·75	0·389	0·0763	0·0377
		2·9	0·547	0·0853	0·0151
		5·05	0·674	0·959	0·0004
		9·35	0·945	0·128	—0·0302
		13·6	1·217	0·188	—0·0761
		15·7	1·324	0·244	—0·0915
		17·75	1·398	0·298	—0·1124
		19·75	1·430	0·380	—0·174
		21·7	1·398	0·454	—0·231
—1·4	0	0·75	0·370	0·0756	0·0750
		2·9	0·499	0·0828	0·0587
		5·05	0·650	0·0952	0·0378
		9·35	0·927	0·126	0·0069
		13·6	1·193	0·187	—0·0377
		15·7	1·305	0·234	—0·0457
		17·75	1·374	0·289	—0·0654
		19·75	1·412	0·362	—0·113
		21·7	1·414	0·450	—0·178
1·5	0	0·75	0·396	0·0763	—0·0012
		5·05	0·682	0·0960	—0·0393
		9·35	0·963	0·130	—0·0737
		13·6	1·237	0·192	—0·1250
		17·75	1·417	0·309	—0·1714

TABLE 10a

Lift, Drag and Pitching-Moment Coefficients on Model B with Body and Fin

No tailplane

α deg	C_L	C_D	$C_{M\,0\cdot45\bar{c}}$
Flaps 0 *deg*			
0·3	0·019	0·0115	0·0014
3·5	0·195	0·0159	0·0162
6·7	0·365	0·0277	0·0335
9·9	0·540	0·0479	0·0503
13·05	0·704	0·0742	0·0643
16·25	0·889	0·116	0·0647
19·4	1·029	0·194	0·0806
21·45	1·057		
22·45	1·073	0·284	0·0988
23·5	1·094	0·316	0·1027
24·5	1·110	0·353	0·1038
25·5	1·22	0·387	0·101
Flaps 60 *deg* (*hinged at* 80 *per cent chord*)			
0·7	0·353	0·0758	—0·0430
3·85	0·524	0·0909	—0·0266
7·05	0·696	0·113	—0·0125
10·25	0·860	0·141	0·0022
13·4	1·018	0·173	0·0140
16·6	1·191	0·220	0·0156
17·55	1·160	0·265	0·0356

TABLE 10b

Lift, Drag and Pitching-Moment Coefficients on Model B with Body and Fin

With tailplane

η_T deg	α deg	C_L	C_D	$C_{M\ 0\cdot 45\bar{c}}$
Flaps 0 deg				
0	0·3	0·025	0·0135	—0·0022
	1·9	0·123	0·0149	—0·0022
	3·5	0·216	0·0189	—0·0071
	6·7	0·404	0·0326	—0·0199
	9·9	0·591	0·0548	—0·0310
	13·05	0·775	0·0853	—0·0481
	15·0	0·914	0·113	—0·0708
	17·25	1·057	0·172	—0·1086
	19·4	1·156	0·230	—0·1338
	21·45	1·218	0·295	—0·1776
	23·5	1·271	0·396	—0·249
	25·5	1·326	0·474	—0·301
—1·4	0·3	0·007	0·0140	0·0301
	3·5	0·194	0·0176	0·0284
	6·7	0·386	0·0309	0·0148
	9·9	0·570	0·0526	0·0009
	13·05	0·765	0·0831	—0·0157
	15·0	0·891	0·111	—0·0367
	17·25	1·022	0·165	—0·0638
	19·4	1·134	0·213	—0·0893
	21·45	1·179	0·303	—0·1432
—2·9	1·4	0·057	0·0140	0·0594
	3·5	0·184	0·0173	0·0578
	6·7	0·368	0·0300	0·0482
	9·9	0·561	0·0515	0·0329
	13·05	0·744	0·0796	0·0183
	15·0	0·883	0·110	—0·0041
	17·25	1·014	0·163	—0·0277
	19·4	1·114	0·207	—0·0464
	21·45	1·163	0·306	—0·1055
Flaps 60 deg (hinged at 80 per cent chord)				
0	0·7	0·309	0·0754	0·0386
	3·85	0·520	0·0901	0·0297
	7·05	0·683	0·112	0·0196
	10·25	0·870	0·142	0·0072
	13·4	1·048	0·181	—0·0137
	15·5	1·181	0·216	—0·0427
	17·55	1·232	0·285	—0·081
	19·55	1·258	0·354	—0·128
	21·55	1·302	0·455	—0·190
	22·55	1·319		
	23·55	1·328	0·531	—0·251

Table 10b—*continued*

η_T deg	α deg	C_L	C_D	$C_{M\,0\cdot45\bar{c}}$
Flaps 60 *deg* (*hinged at* 80 *per cent chord*)—*continued*				
−1·4	0·7	0·289	0·0745	0·0699
	3·85	0·488	0·0894	0·0567
	7·05	0·671	0·111	0·0477
	10·25	0·852	0·141	0·0369
	13·4	1·028	0·177	0·0197
	15·5	1·163	0·212	−0·0084
	17·55	1·224	0·280	−0·041
	19·55	1·232	0·350	−0·087
	21·55	1·281	0·442	−0·135
	23·55	1·317	0·517	−0·202
	25·55	1·348	0·593	−0·263
−2·9	10·25	0·835	0·141	0·0698
	13·4	1·021	0·177	0·0494
	15·5	1·137	0·206	0·0275
	17·55	1·187	0·246	−0·007
	19·55	1·212	0·343	−0·044
1·5	0·7	0·331	0·0754	0·0063
	3·85	0·514	0·0903	−0·0050
	7·05	0·695	0·115	−0·0163
	10·25	0·877	0·144	−0·0296
	13·4	1·058	0·183	−0·0543
	15·5	1·194	0·218	−0·0856
	17·55	1·245	0·289	−0·130
	19·55	1·275	0·384	−0·188

TABLE 11

Lateral and Directional Coefficients and Derivatives on Model A with Body

$C_L = 0$ Flaps 0 deg

(c.g. at $0{\cdot}45\bar{c}$)

β deg	$10^3 C_n$	$10^3 C_Y$	n_v	y_v
No fin or tailplane				
2·5	−2·85	−2·81	−0·065	−0·032
5	−5·48	−6·13		
10	−8·88	−16·56		
With fin and tailplane $\eta_T = 0$ deg				
2·5	4·10	−15·11	0·094	−0·173
5	8·37	−30·63		
10	18·32	−65·36		

TABLE 12

Lateral and Directional Coefficients and Derivatives on Model B with Body

$C_L = 0$ Flaps 0 deg

(c.g. at $0{\cdot}45\bar{c}$)

β deg	$10^3 C_n$	$10^3 C_Y$	$10^3 C_l$	n_v	y_v	l_v
No fin or tailplane						
2·5	−3·34	−1·85	−0·49	−0·077	−0·021	−0·011
5	−6·45	−4·55	−0·91			
10	−10·91	−13·6	−1·47			
With fin and tailplane. $\eta_T = 0$ deg						
2·5	4·82	−12·9	−1·07	0·110	−0·148	−0·025
5	9·85	−26·7	−2·61			
10	21·60	−55·6	−5·15			

TABLE 13a

Flat Plate Type Nose Flaps on Model A

Lift, Drag and Pitching-Moment Coefficients on the Wing alone, *i.e.*, with no Body or Tail Unit

Flaps 0 deg				Flaps 60 deg (hinged at 80 per cent chord)			
α deg	C_L	C_D	$C_{M\,0\cdot25\bar{c}}$	α deg	C_L	C_D	$C_{M\,0\cdot25\bar{c}}$
50 *per cent span nose flaps.* $\eta_W = 0$ *deg*							
0·3	−0·012	0·0228	+0·0037				
4·6	+0·279	0·0208	−0·0293				
8·9	0·536	0·0351	−0·0471				
13·15	0·771	0·0645	−0·0570				
15·3	0·897	0·0918	−0·0655				
17·45	1·002	0·1290	−0·0559				
19·5	1·080	0·1728	−0·0426				
21·6	1·152	0·2231	−0·0199				
23·65	1·218	0·2829	−0·0038				
25·75	1·284						
26·75	1·280						
40 *per cent span nose flaps.* $\eta_W = 0$ *deg*							
4·6	0·275	0·0189	−0·0261	5·2	0·800	0·1204	−0·1261
8·9	0·521	0·0336	−0·0475	9·45	1·044	0·1531	−0·1446
13·15	0·764	0·0621	−0·0605	13·75	1·268	0·2052	−0·1561
15·3	0·884	0·0909	−0·0687	15·7	1·345	0·2551	−0·1439
17·4	0·988	0·1281	−0·0642	17·8	1·310	0·3167	−0·1173
19·55	1·093	0·1777	−0·0611				
21·6	1·167	0·2271	−0·0379				
23·65	1·219	0·2725	−0·0238				
25·7	1·259	0·3759	−0·0468				

TABLE 13b

Curved Surface Type Nose Flaps on Model A

Lift, Drag and Pitching-Moment Coefficients on the Wing Alone and Wing and Body (no Tail Unit)

Flaps 0 deg				Flaps 60 deg (hinged at 80 per cent chord)			
α deg	C_L	C_D	$C_{M\,0\cdot25\bar{c}}$	α deg	C_L	C_D	$C_{M\,0\cdot25\bar{c}}$
Wing alone with 50 per cent span nose flaps. $\eta_W = 0$ *deg*							
0·3	−0·021	0·0206	+0·0057	9·5	1·057	0·1526	−0·1517
4·6	+0·266	0·0187	−0·0271	13·75	1·278	0·1983	−0·1638
8·9	0·527	0·0334	−0·0467	15·85	1·383	0·2401	−0·1617
13·15	0·766	0·0589	−0·0573	16·9	1·421	0·2615	−0·1486
15·3	0·893	0·0832	−0·0668	17·9	1·437	0·2843	−0·1286
17·45	1·013	0·1197	−0·0804	19·8	1·333	0·3680	−0·0573
19·55	1·122	0·1635	−0·0835				
20·6	1·131	0·2000	−0·0508				
21·6	1·149	0·2280	−0·0266				
23·65	1·199	0·2764	−0·0015				
25·7	1·239						
26·7	1·257						
27·75	1·265						
Wing alone with 50 per cent span nose flaps. $\eta_W = -10$ *deg*							
				9·35	0·953	0·1472	−0·0743
				13·65	1·208	0·1922	−0·0053
				15·8	1·310	0·2290	−0·1077
				17·8	1·342	0·2794	−0·0730
				19·75	1·273	0·3554	−0·0250
Wing alone with 50 per cent span nose flaps and inboard fin. $\eta_W = 0$ *deg.*							
8·9	0·550	0·0356	−0·0527	9·5	1·044	0·1525	−0·1431
13·2	0·785	0·0618	−0·0691	13·75	1·283	0·2015	−0·1614
15·35	0·926	0·0852	−0·0845	15·85	1·388	0·2404	−0·1640
17·5	1·052	0·1200	−0·1119	17·8	1·341	0·3012	−0·1487
19·55	1·091	0·1920	−0·1047				
21·55	1·127	0·2364	−0·0985				
23·6	1·164	0·2766	−0·0825				
Wing alone with 40 per cent span nose flaps. $\eta_W = 0$ *deg*							
8·9	0·525	0·0323	−0·0471	9·5	1·043	0·1500	−0·1511
13·15	0·765	0·0589	−0·0590	13·7	1·259	0·1974	−0·1642
15·3	0·876	0·0817	−0·0645	15·85	1·374	0·2455	−0·1647
17·45	1·004	0·1191	−0·0819	16·8	1·350	0·2830	−0·1424
19·5	1·084	0·1741	−0·0721	17·8	1·336	0·3102	−0·1141
21·6	1·161	0·2251	−0·0334				
23·65	1·208						
25·7	1·226						
27·7	1·260						
Wing and body with 50 per cent span nose flaps. $\eta_W = 0$ *deg*							
8·95	0·558	0·0418	−0·054	9·35	0·924	0·125	−0·165
13·25	0·821	0·0756	−0·070	13·65	1·178	0·172	−0·183
16·45	1·014	0·125	−0·091	15·75	1·287	0·213	−0·182
18·55	1·120	0·167	−0·087	17·8	1·343	0·261	−0·151
19·6	1·158	0·199	−0·072	19·8	1·320	0·323	−0·095
21·65	1·186	0·254	−0·028				
23·65	1·215	0·312	0·012				

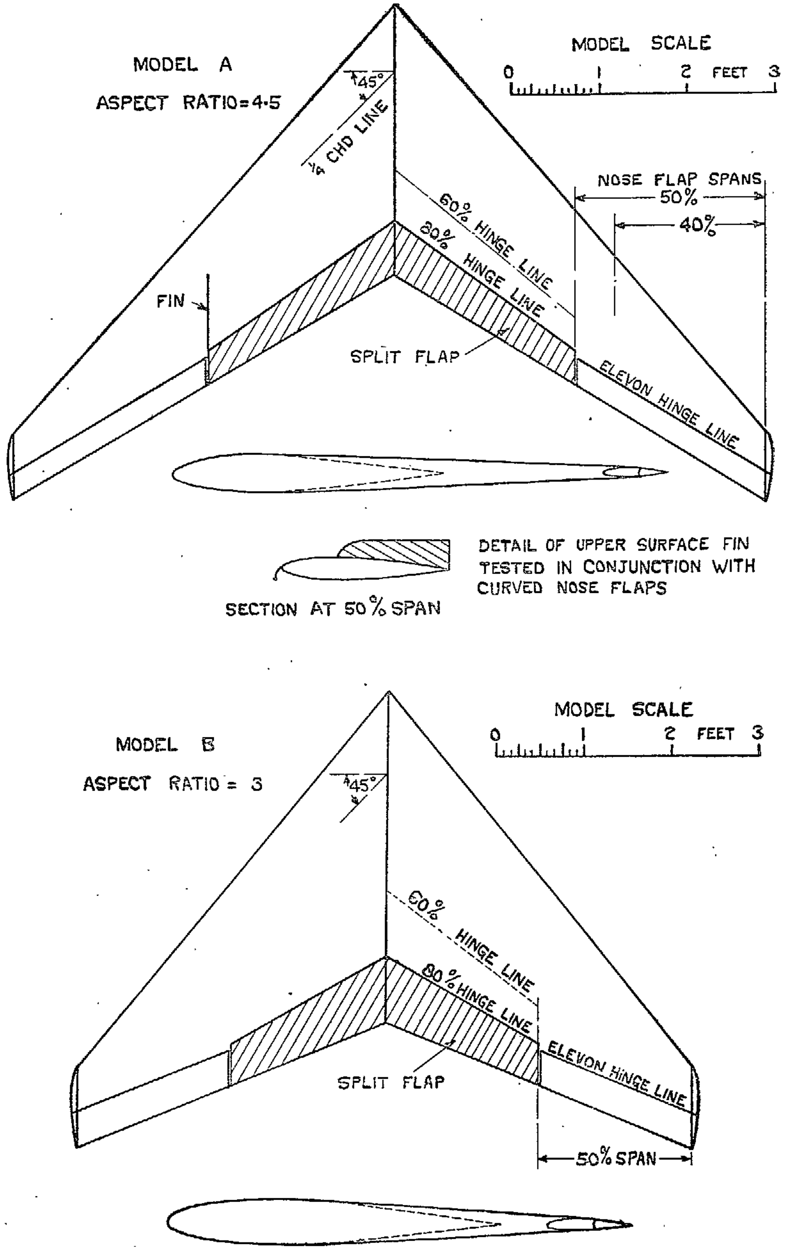

FIGS. 1a and b. Models A and B. Wing planforms.

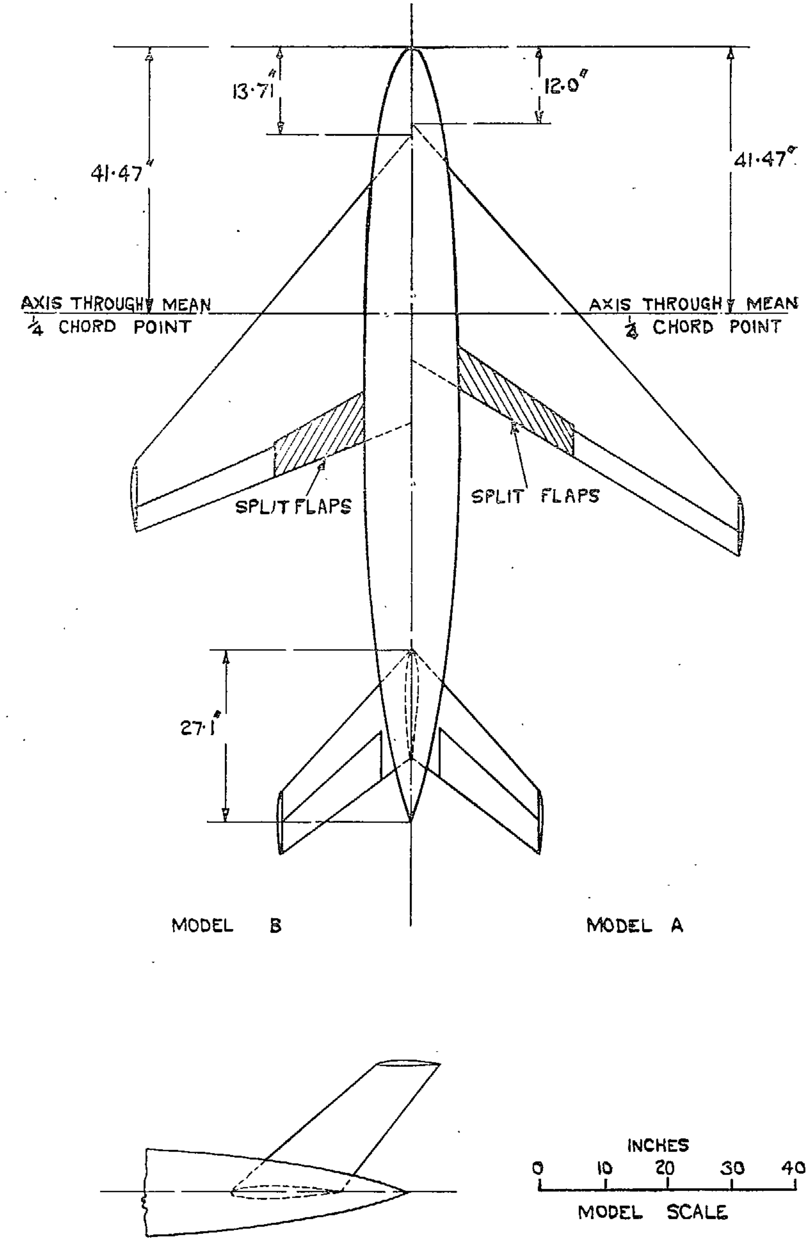

FIG. 2. General arrangement of body and tail unit tested on models A and B.

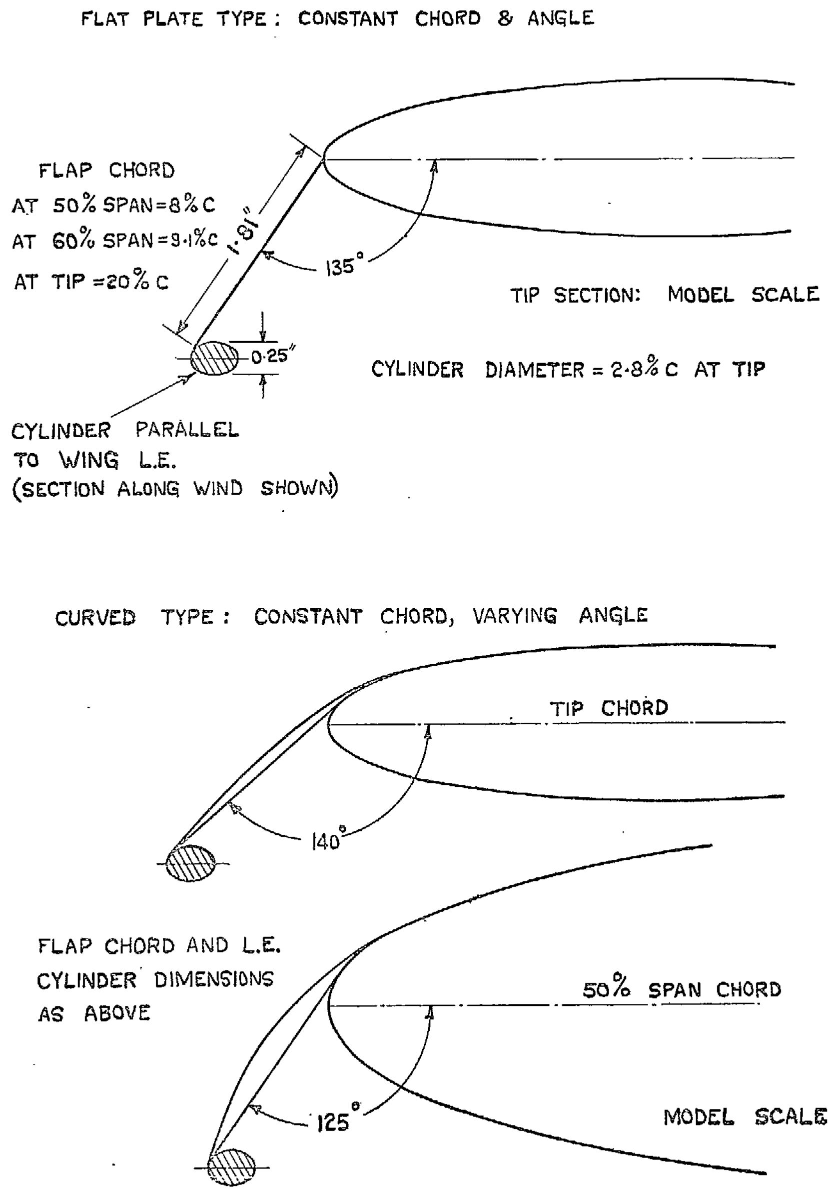

FIGS. 3a and 3b. Model A : nose flap details.

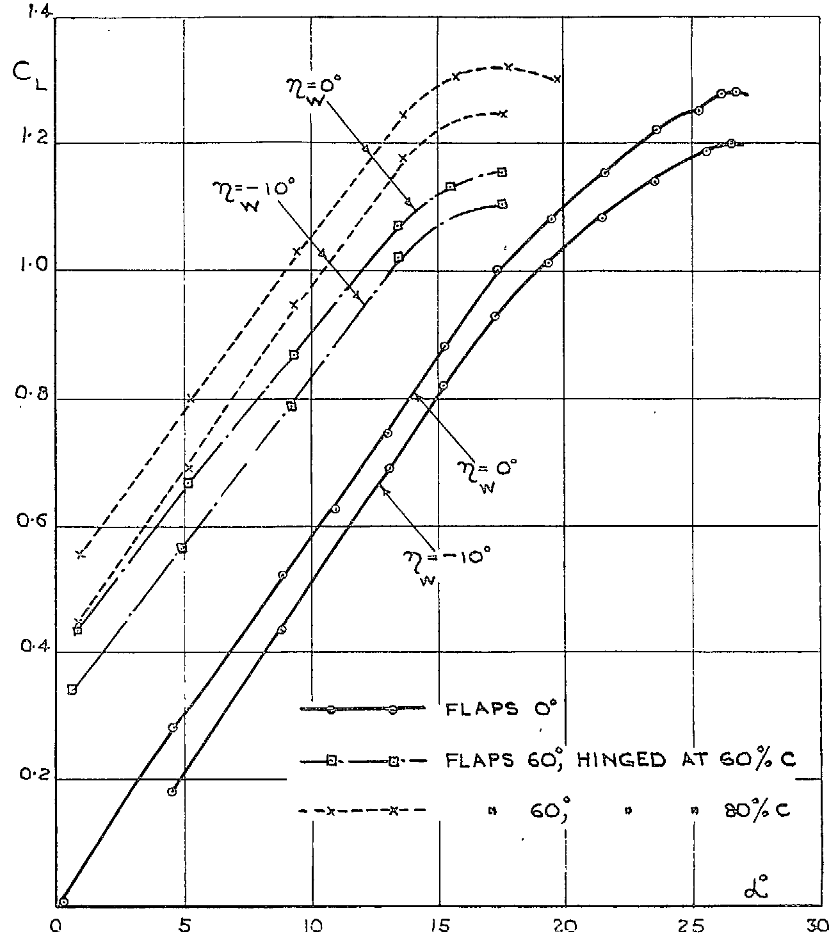

FIG. 4. Model A. Lift coefficients, wing alone (aspect ratio = 4·5).

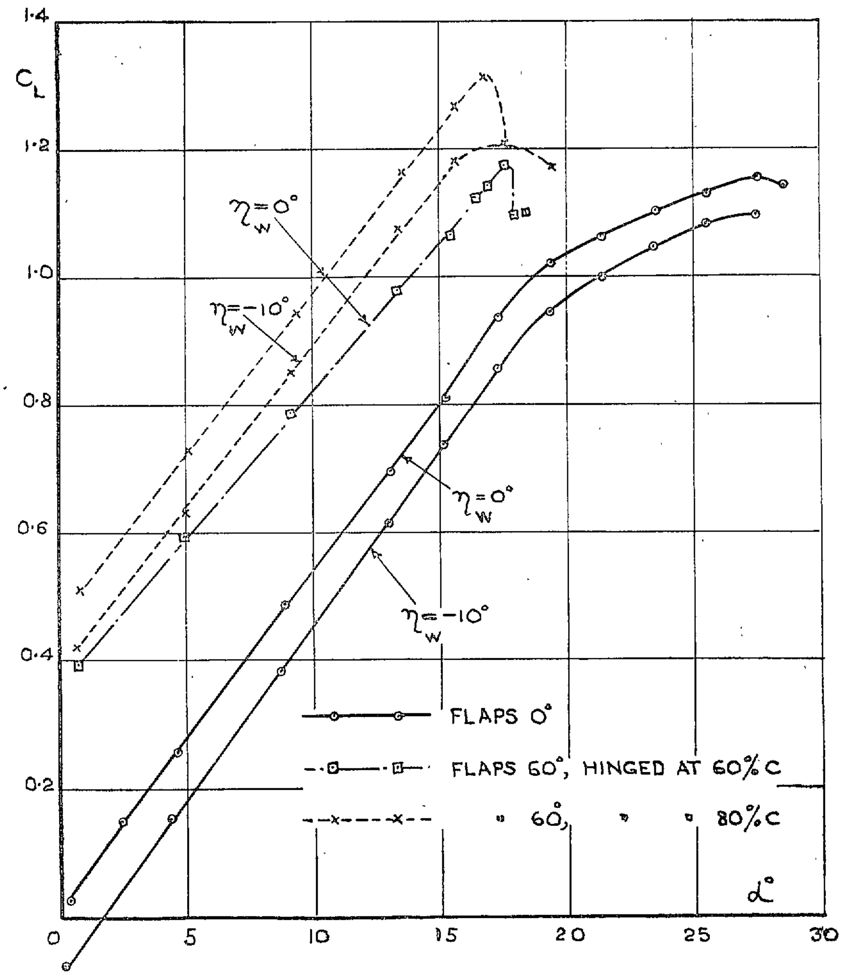

FIG. 5. Model B. Lift coefficients, wing alone (aspect ratio = 3·0).

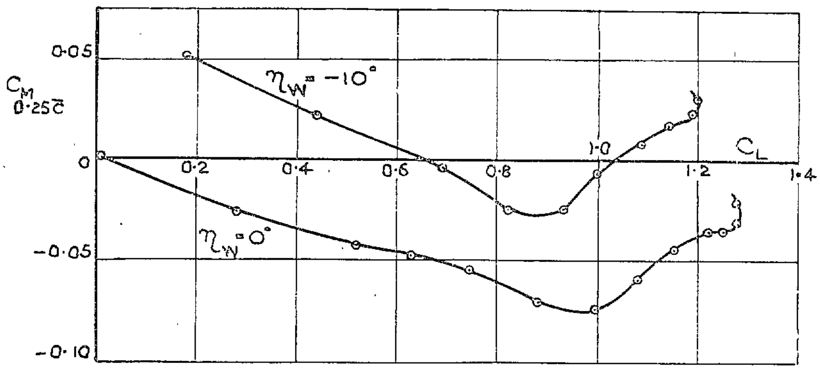

FIG. 6. Flaps 0 deg.

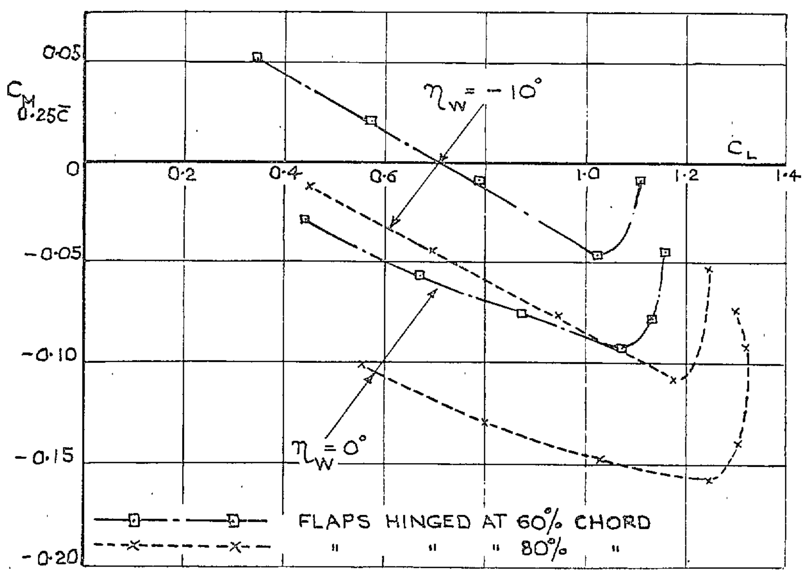

FIG. 7. Flaps 60 deg.

FIGS. 6 and 7. Model A. Pitching moments, wing alone (aspect ratio = 4·5).

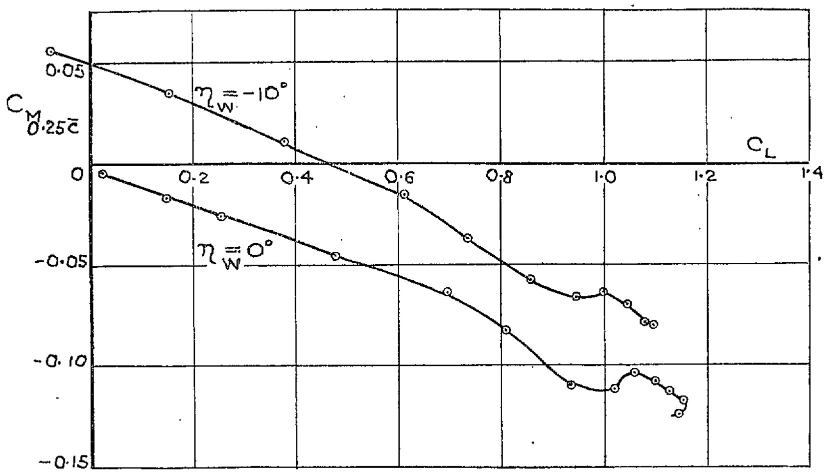

FIG. 8. Flaps 0 deg.

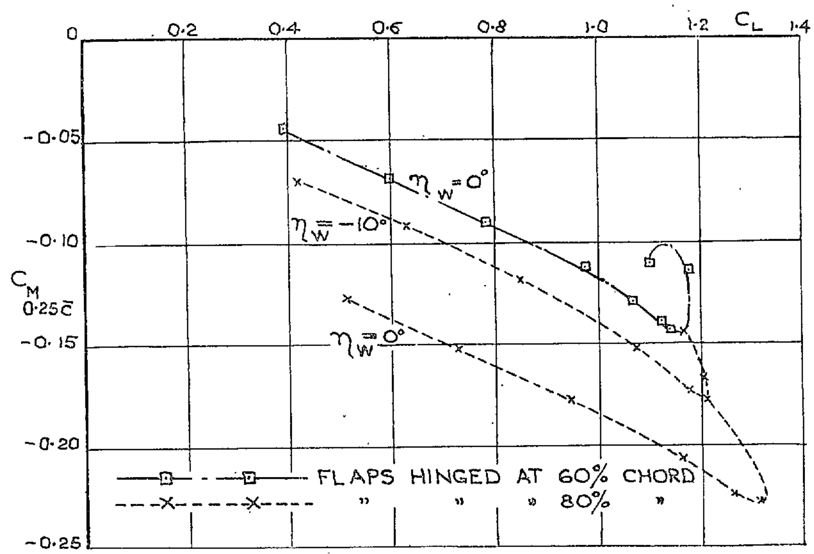

FIG. 9. Flaps 60 deg.

FIGS. 8 and 9. Model B. Pitching moments, wing alone (aspect ratio = 3·0).

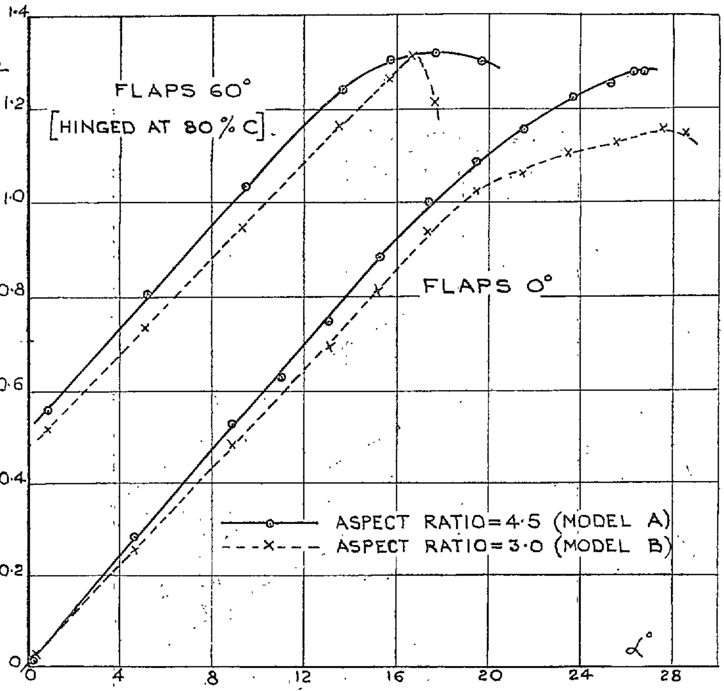

FIG. 10. Lift coefficients $\eta_W = 0$ deg.

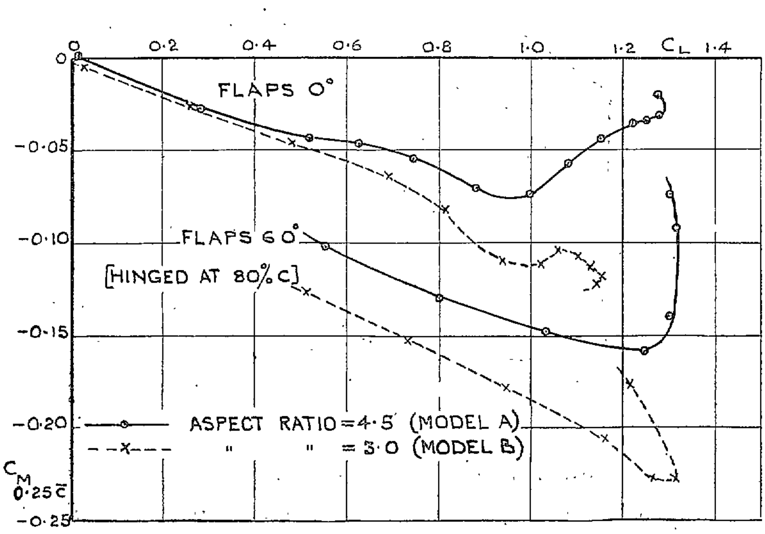

FIG. 11. Pitching moments $\eta_W = 0$ deg.

FIGS. 10 and 11. Effect of aspect ratio on longitudinal stability. Wing alone.

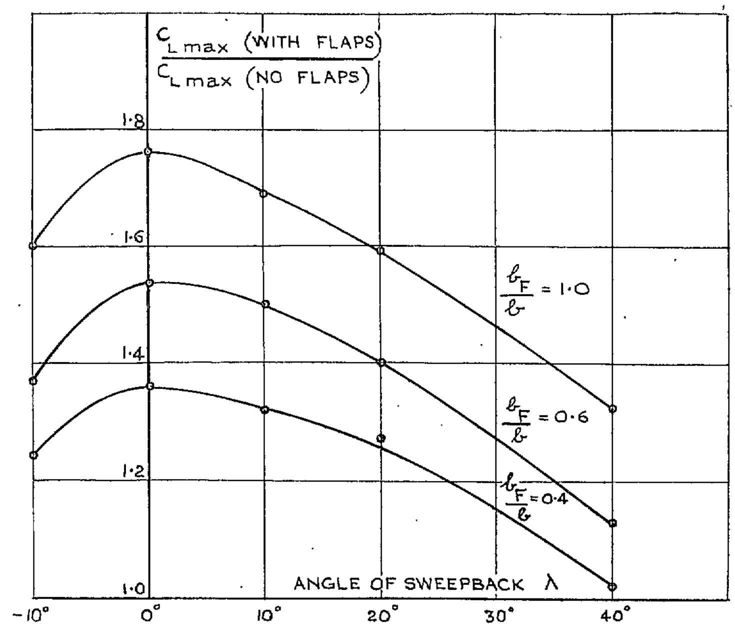

$\Delta C_{L\ max}$ DUE TO FLAPS FOR RANGE OF SWEEPBACK ANGLES

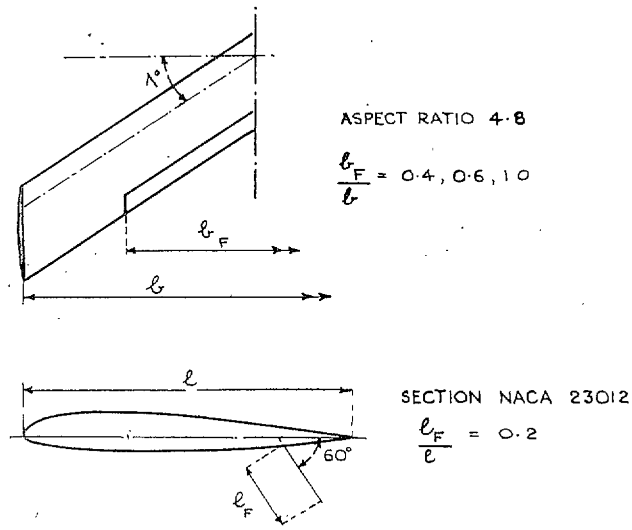

WING PLANFORM AND SECTION

FIG. 12. Extract from German report on split flaps (Ref. 2).

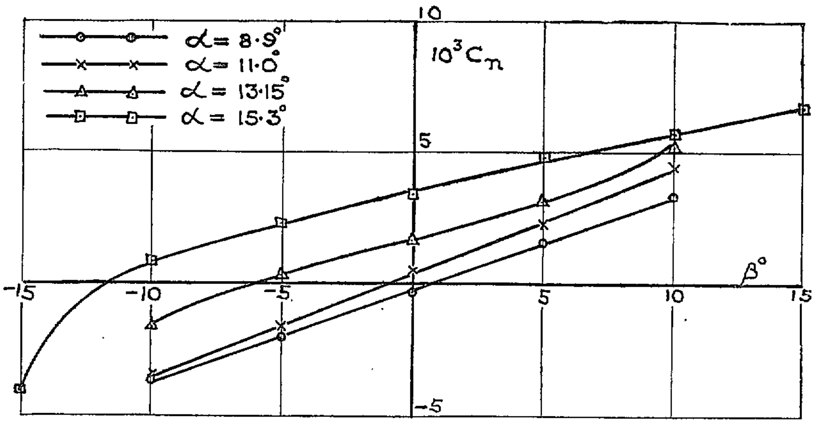

FIG. 13. Model A (aspect ratio = 4·5).

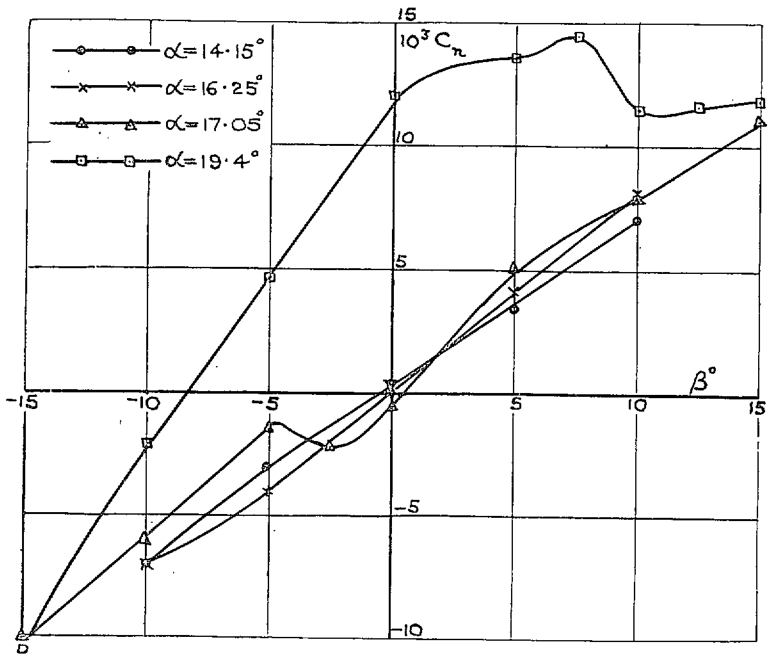

FIG. 14. Model B (aspect ratio = 3·0).

FIGS. 13 and 14. Yawing moments. Wing alone, flaps 0 deg.

C1

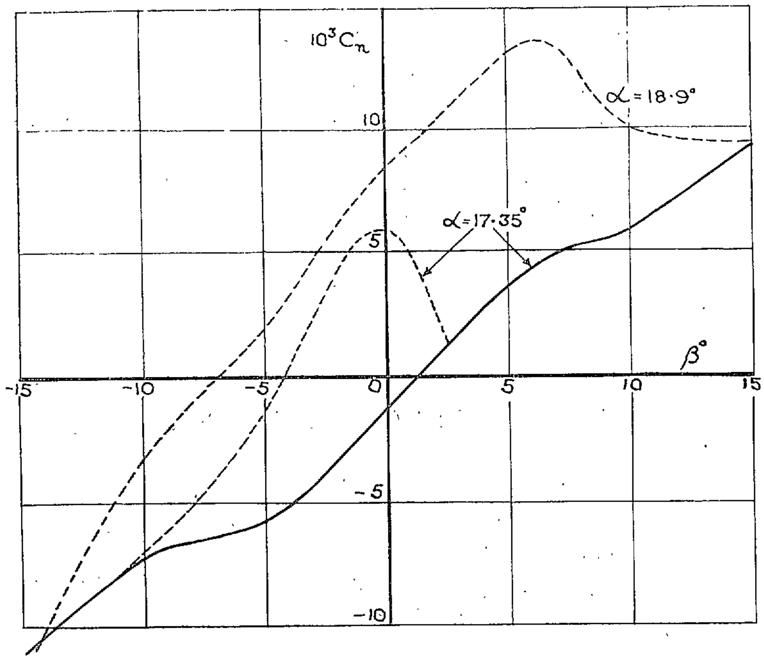

FIG. 15. Yawing moments.

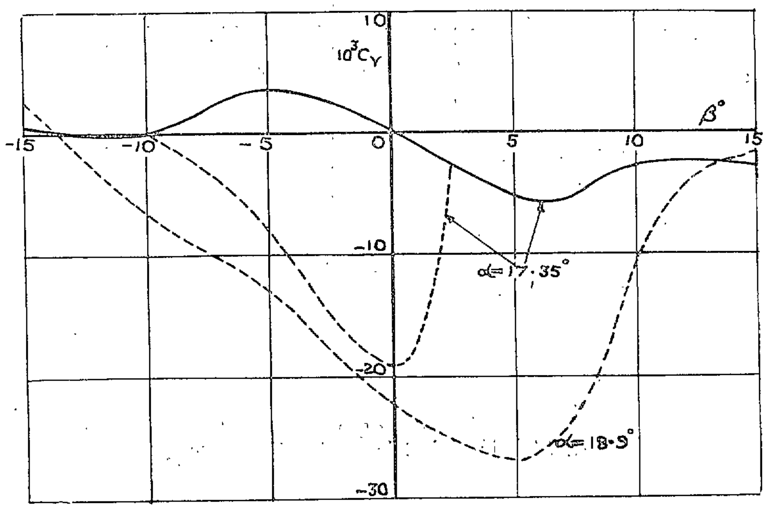

FIG. 16. Sideforce.

FIGS. 15 and 16. Model B. Wing alone. Extract from Ref. 4.

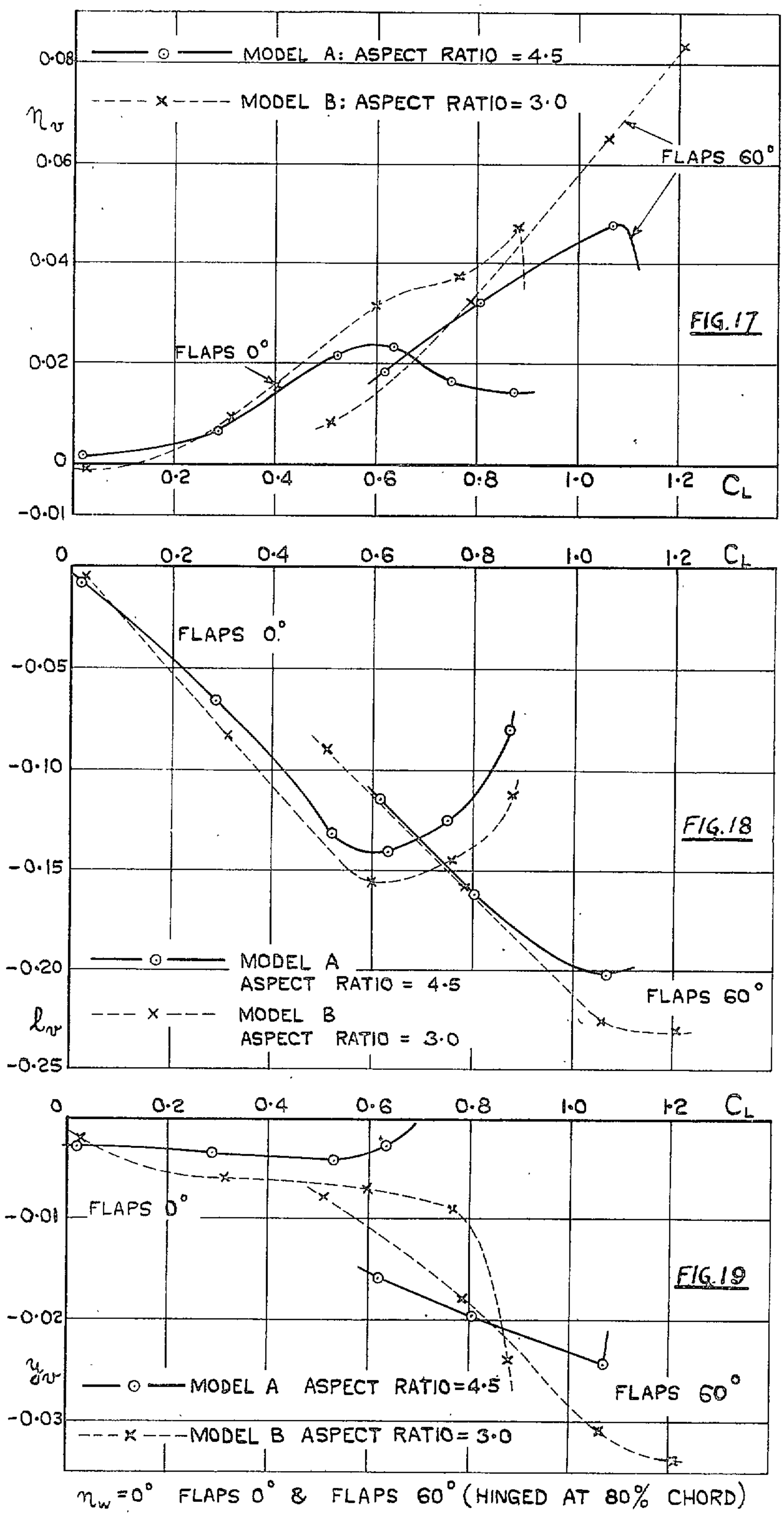

FIGS. 17, 18 and 19. Effect of aspect ratio on n_v, l_v and y_v. Wing alone.

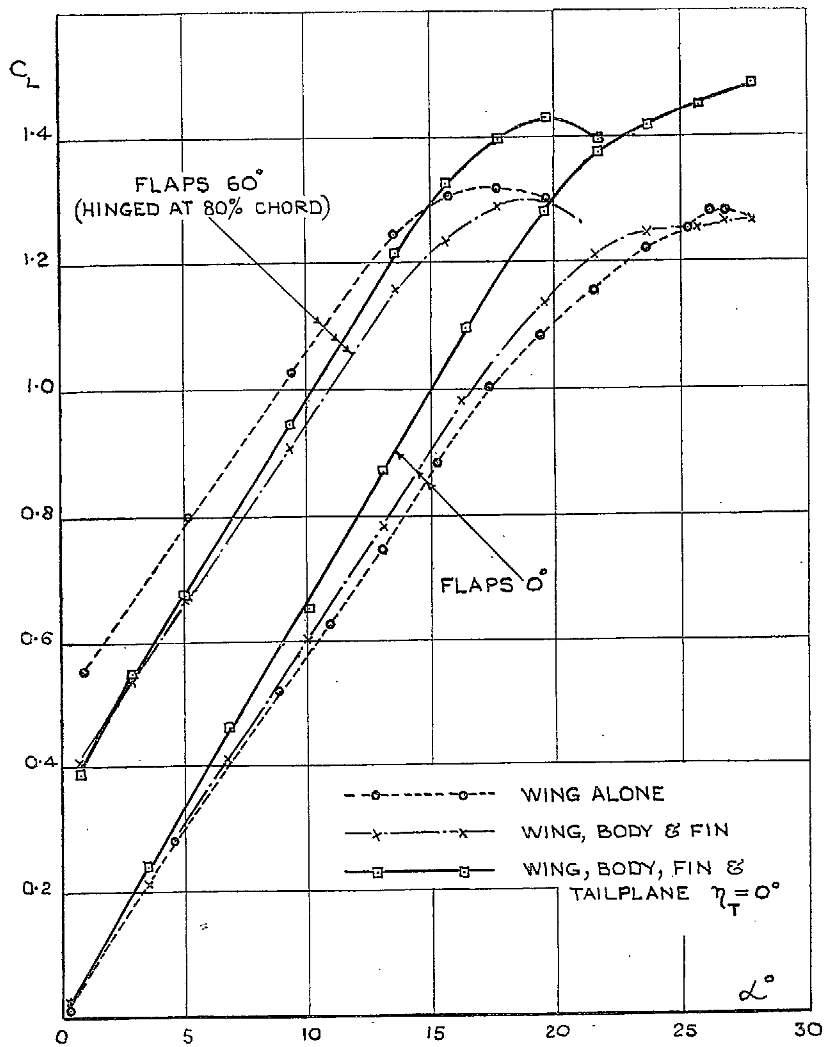

FIG. 20. Model A. Lift coefficients. Effect of body and tailplane (aspect ratio = 4·5).

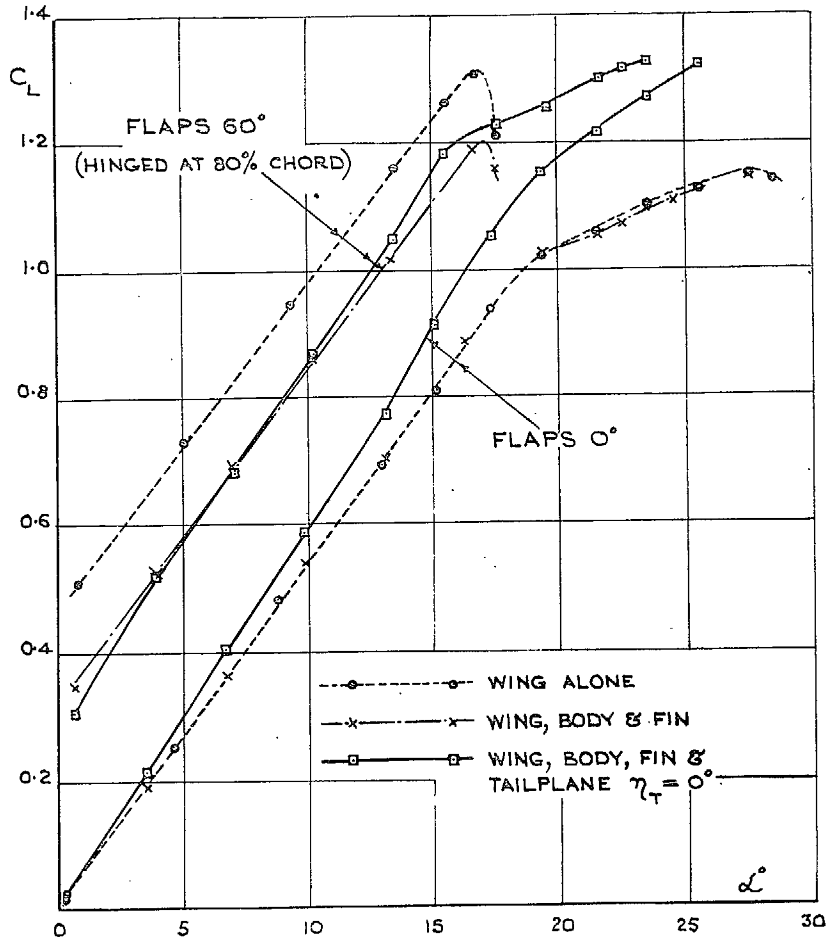

FIG. 21. Model B. Lift coefficients. Effect of body and tailplane (aspect ratio = 3·0).

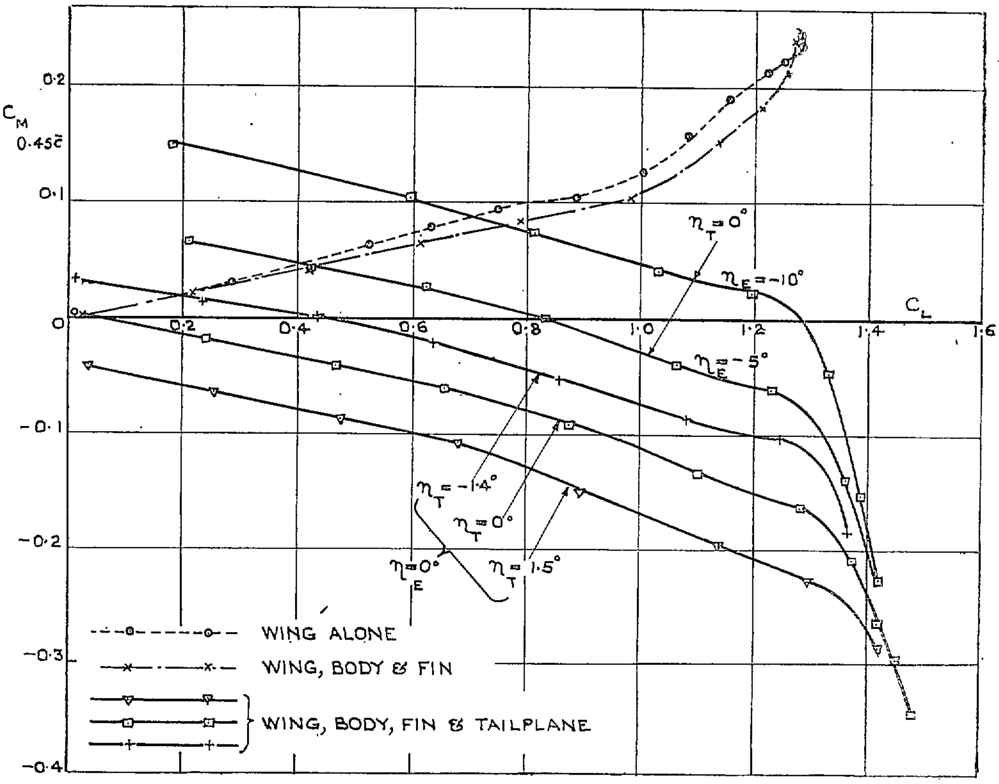

FIG. 22. Model A. Pitching moments, flaps 0 deg (aspect ratio = 4·5).

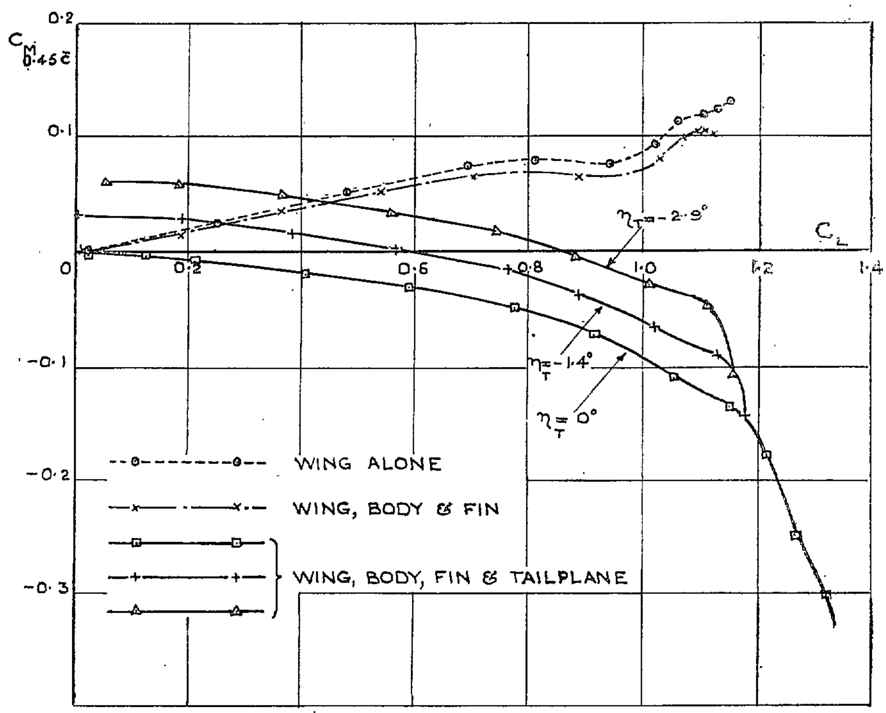

FIG. 23. Model B. Pitching moments, flaps 0 deg (aspect ratio = 3·0).

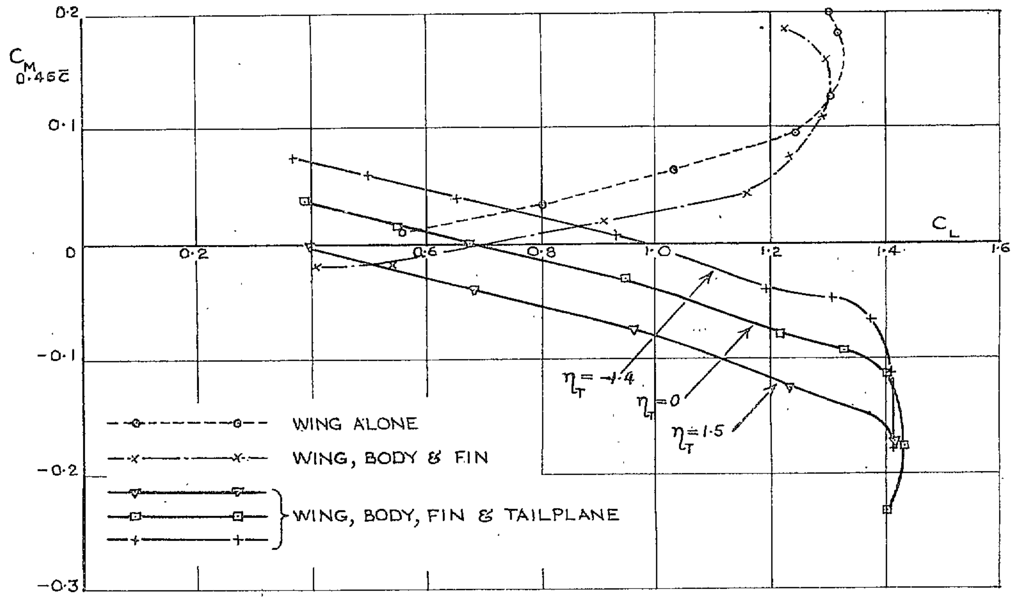

FIG. 24. Model A. Pitching moments, flaps 60 deg (flaps hinged at 80 per cent chord, aspect ratio = 4·5).

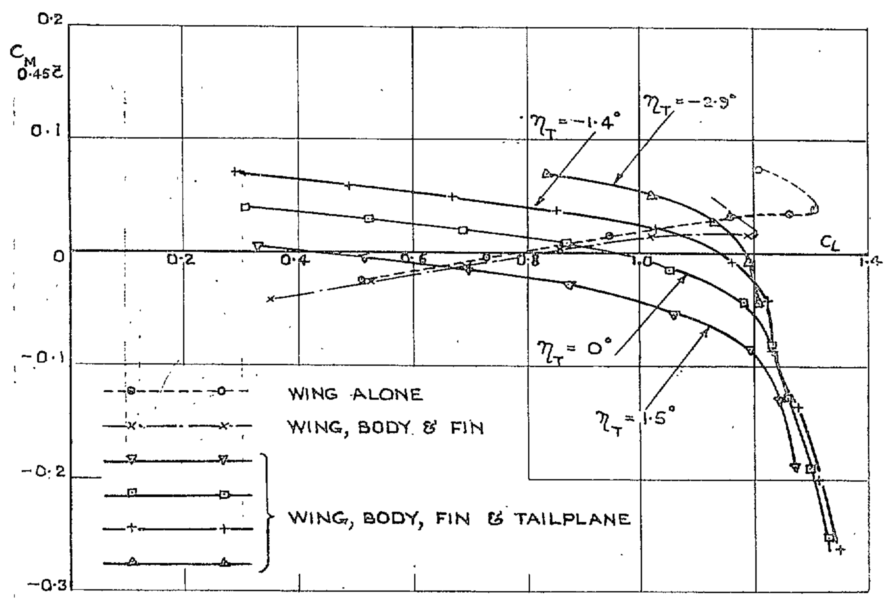

FIG. 25. Model B. Pitching moments, flaps 60 deg (flaps hinged at 80 per cent chord, aspect ratio = 3·0).

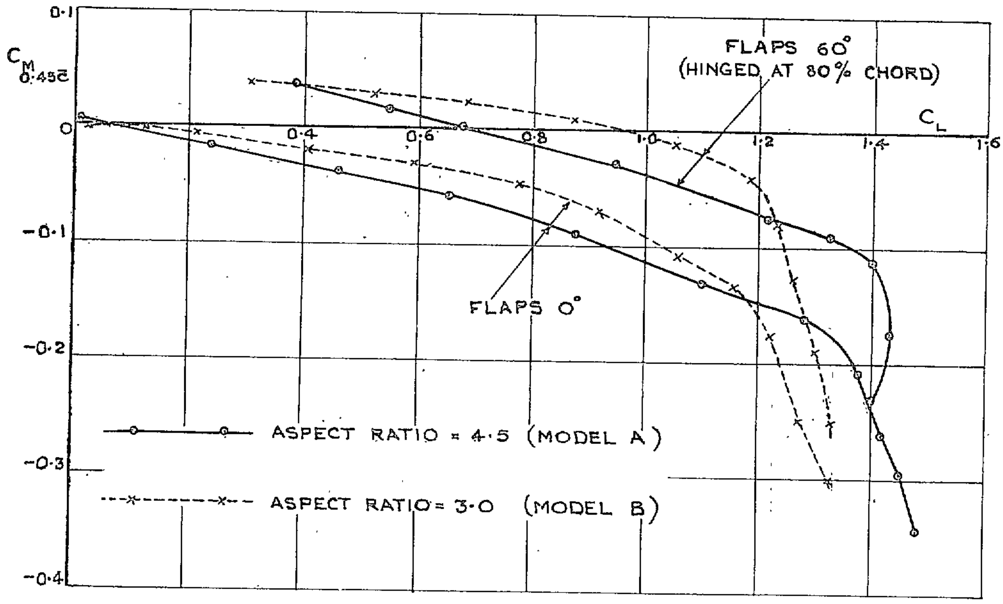

FIG. 26. Effect of aspect ratio on longitudinal stability (wing, body and tail results).

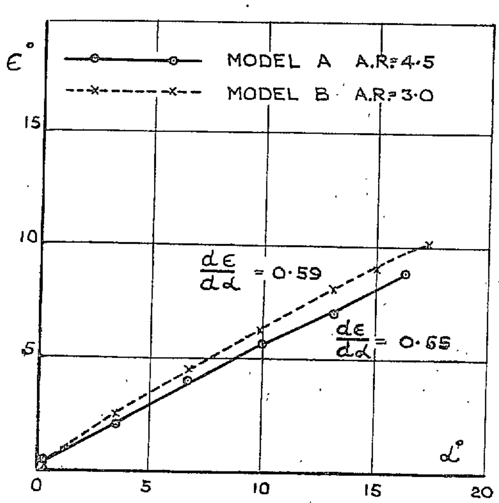

FIG. 27. Flaps 0 deg.

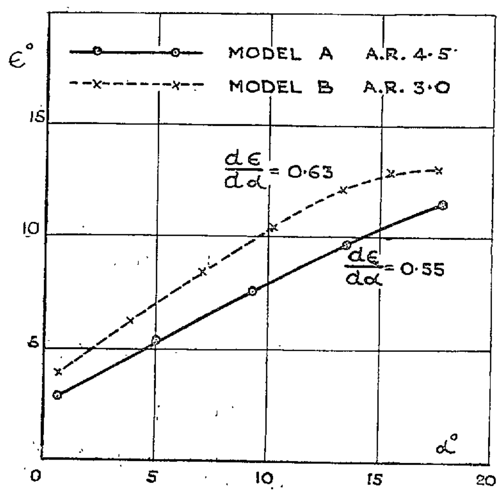

FIG. 28. Flaps 60 deg (hinged at 80 per cent chord).

FIGS. 27 and 28. Downwash curves.

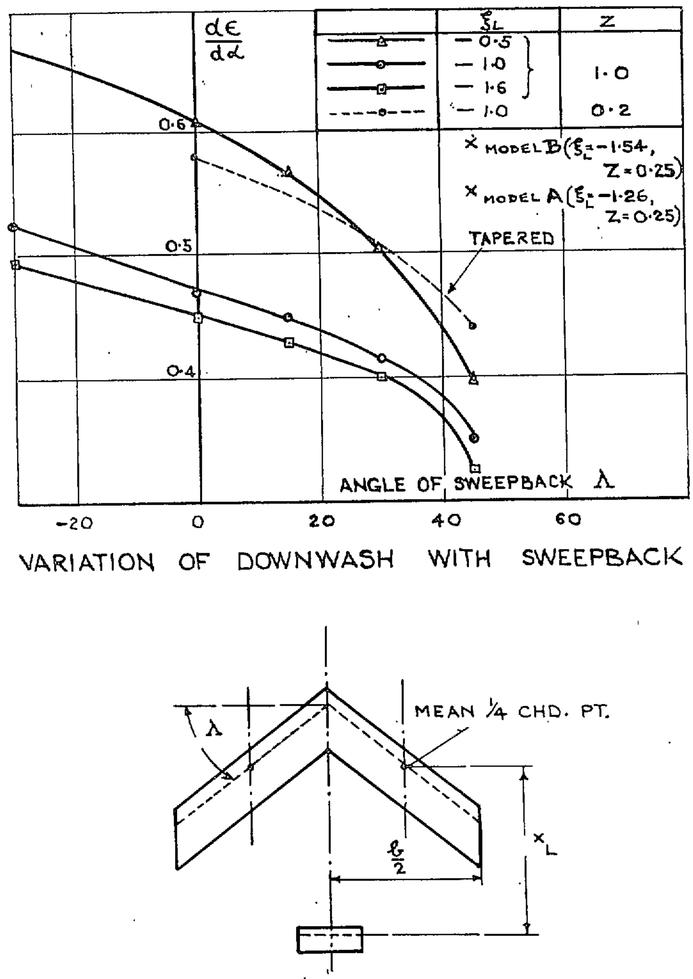

WING DETAILS . ASPECT RATIO 5·0
SECTION NACA 23012
TAILPLANE SECTION NACA 0015

$-x_L$ = DISTANCE OF ¼ CHORD TAILPLANE AFT OF WING MEAN ¼ CHORD POINT.

$\xi_L = x_L / \left(\frac{b}{2}\right)$

Z = TAPER RATIO $\left(\frac{\text{TIP CHORD}}{\text{ROOT CHORD}}\right)$

THE TAILPLANE HEIGHT IS ZERO IN ALL CASES

FIG. 29. Extract from T.N. No. Aero 1819.

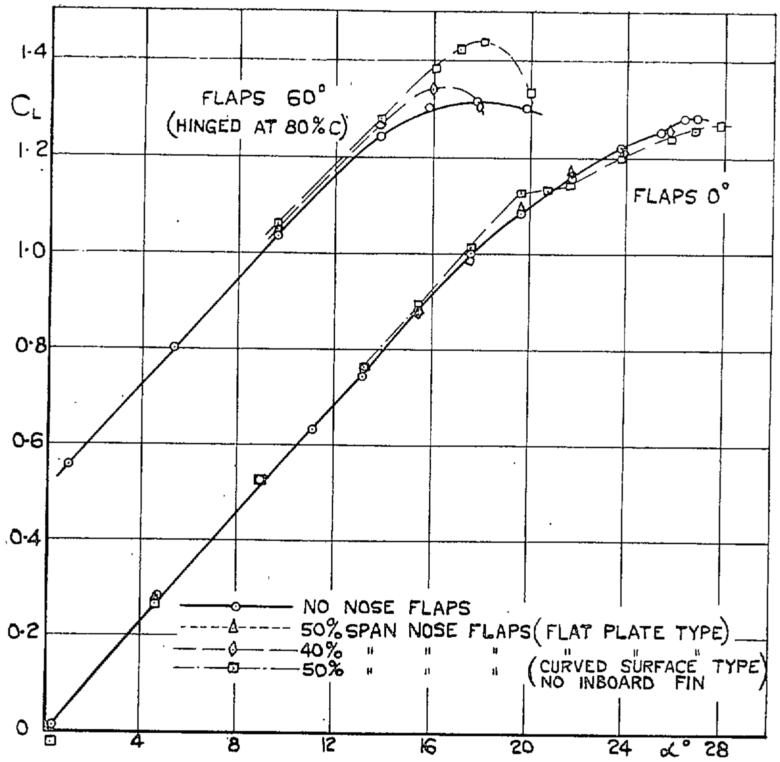

FIG. 30. Lift coefficients. $\eta_W = 0$ deg.

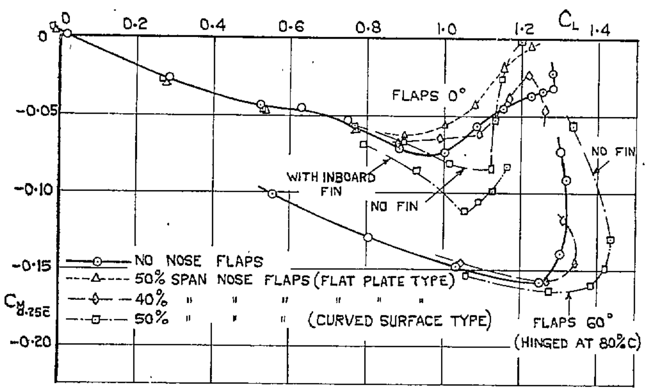

FIG. 31. Pitching moments. $\eta_W = 0$ deg.

FIGS. 30 and 31. Effect of nose flaps on Model A.

J4264 Wt.13/806 K9 4/53 D&Co. 34-263

PRINTED IN GREAT BRITAIN

R. & M. No. 2710
(10,904)
A.R.C. Technical Report

Publications of the Aeronautical Research Council

ANNUAL TECHNICAL REPORTS OF THE AERONAUTICAL RESEARCH COUNCIL (BOUND VOLUMES)

1936 Vol. I. Aerodynamics General, Performance, Airscrews, Flutter and Spinning. 40s. (40s. 9d.)
Vol. II. Stability and Control, Structures, Seaplanes, Engines, etc. 50s. (50s. 10d.)

1937 Vol. I. Aerodynamics General, Performance, Airscrews, Flutter and Spinning. 40s. (40s. 10d.)
Vol. II. Stability and Control, Structures, Seaplanes, Engines, etc. 60s. (61s.)

1938 Vol. I. Aerodynamics General, Performance, Airscrews. 50s. (51s.)
Vol. II. Stability and Control, Flutter, Structures, Seaplanes, Wind Tunnels, Materials. 30s. (30s. 9d.)

1939 Vol. I. Aerodynamics General, Performance, Airscrews, Engines. 50s. (50s. 11d.)
Vol. II. Stability and Control, Flutter and Vibration, Instruments, Structures, Seaplanes, etc. 63s. (64s. 2d.)

1940 Aero and Hydrodynamics, Aerofoils, Airscrews, Engines, Flutter, Icing, Stability and Control, Structures, and a miscellaneous section. 50s. (51s.)

1941 Aero and Hydrodynamics, Aerofoils, Airscrews, Engines, Flutter, Stability and Control, Structures. 63s. (64s. 2d.)

1942 Vol. I. Aero and Hydrodynamics, Aerofoils, Airscrews, Engines. 75s. (76s. 3d.)
Vol. II. Noise, Parachutes, Stability and Control, Structures, Vibration, Wind Tunnels. 47s. 6d. (48s. 5d.)

1943 Vol. I. (*In the press.*)
Vol. II. (*In the press.*)

ANNUAL REPORTS OF THE AERONAUTICAL RESEARCH COUNCIL—

1933–34	1s. 6d. (1s. 8d.)	1937	2s. (2s. 2d.)
1934–35	1s. 6d. (1s. 8d.)	1938	1s. 6d. (1s. 8d.)
April 1, 1935 to Dec. 31, 1936.	4s. (4s. 4d.)	1939–48	3s. (3s. 2d.)

INDEX TO ALL REPORTS AND MEMORANDA PUBLISHED IN THE ANNUAL TECHNICAL REPORTS, AND SEPARATELY—

April, 1950 - - - - R. & M. No. 2600. 2s. 6d. (2s. 7½d.)

AUTHOR INDEX TO ALL REPORTS AND MEMORANDA OF THE AERONAUTICAL RESEARCH COUNCIL—

1909–1949 - - - - - R. & M. No. 2570. 15s. (15s. 3d.)

INDEXES TO THE TECHNICAL REPORTS OF THE AERONAUTICAL RESEARCH COUNCIL—

December 1, 1936 — June 30, 1939.	R. & M. No. 1850.	1s. 3d. (1s. 4½d.)
July 1, 1939 — June 30, 1945.	R. & M. No. 1950.	1s. (1s. 1½d.)
July 1, 1945 — June 30, 1946.	R. & M. No. 2050.	1s. (1s. 1½d.)
July 1, 1946 — December 31, 1946.	R. & M. No. 2150.	1s. 3d. (1s. 4½d.)
January 1, 1947 — June 30, 1947.	R. & M. No. 2250.	1s. 3d. (1s. 4½d.)
July, 1951 - - - -	R. & M. No. 2350.	1s. 9d. (1s. 10½d.)

Prices in brackets include postage.

Obtainable from

HER MAJESTY'S STATIONERY OFFICE

York House, Kingsway, London W.C.2 ; 423 Oxford Street, London W.1 (Post Orders : P.O. Box No. 569, London S.E.1) ; 13A Castle Street, Edinburgh 2 ; 39 King Street, Manchester 2 ; 2 Edmund Street, Birmingham 3 ; 1 St. Andrew's Crescent, Cardiff ; Tower Lane, Bristol 1 ; 80 Chichester Street, Belfast OR THROUGH ANY BOOKSELLER

S.O. Code No. 23-2710